

# 1 Highly oxygenated organic molecules (HOM) formation in the 2 isoprene oxidation by $\text{NO}_3$ radical

3 Defeng Zhao<sup>1, 2, 3, 4</sup>, Iida Pullinen<sup>2, a</sup>, Hendrik Fuchs<sup>2</sup>, Stephanie Schrade<sup>2</sup>, Rongrong Wu<sup>2</sup>, Ismail-Hakki Acir<sup>2, b</sup>, Ralf  
4 Tillmann<sup>2</sup>, Franz Rohrer<sup>2</sup>, Jürgen Wildt<sup>2</sup>, Yindong Guo<sup>1</sup>, Astrid Kiendler-Scharr<sup>2</sup>, Andreas Wahner<sup>2</sup>, Sungah Kang<sup>2</sup>, Luc  
5 Vereecken<sup>2</sup>, Thomas F. Mentel<sup>2</sup>

6 <sup>1</sup>Department of Atmospheric and Oceanic Sciences & Institute of Atmospheric Sciences, Fudan University, Shanghai,  
7 200438, China;

8 <sup>2</sup>Institute of Energy and Climate Research, IEK-8: Troposphere, Forschungszentrum Jülich, 52425, Jülich, Germany

9 <sup>3</sup>Big Data Institute for Carbon Emission and Environmental Pollution, Fudan University, Shanghai, 200438, China

10 <sup>4</sup>Institute of Eco-Chongming (IEC), 20 Cuiniao Rd., Chenjia Zhen, Chongming, Shanghai 202162, China

11 <sup>a</sup>Now at: Department of Applied Physics, University of Eastern Finland, Kuopio, 7021, Finland.

12 <sup>b</sup>Now at: Institute of Nutrition and Food Sciences, University of Bonn, Bonn, 53115, Germany;

13 *Correspondence to:* Thomas F. Mentel (t.mentel@fz-juelich.de), Defeng Zhao (dfzhao@fudan.edu.cn)

## 14 Abstract

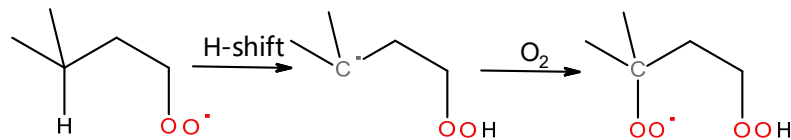
15 Highly oxygenated organic molecules (HOM) are found to play an important role in the formation and  
16 growth of secondary organic aerosol (SOA). SOA is an important type of aerosol with significant impact on air  
17 quality and climate. Compared with the oxidation of volatile organic compounds by ozone ( $\text{O}_3$ ) and hydroxyl radical  
18 ( $\text{OH}$ ), HOM formation in the oxidation by nitrate  $\text{NO}_3$ -radical ( $\text{NO}_3$ ), an important oxidant at night-time and dawn,  
19 has received less attention. In this study, HOM formation in the reaction of isoprene with  $\text{NO}_3$  was investigated in  
20 the SAPHIR chamber (Simulation of Atmospheric PHotochemistry In a large Reaction chamber). A large number of  
21 HOM including monomers ( $\text{C}_5$ ), dimers ( $\text{C}_{10}$ ), and trimers ( $\text{C}_{15}$ ), both closed-shell compounds and open-shell peroxy  
22 radicals ( $\text{RO}_2$ ), were identified and were classified into various series according to their formula. Their formation  
23 pathways were proposed based on the peroxy radicals observed and known mechanisms in the literature, which were  
24 further constrained by the time profiles of HOM after sequential isoprene addition to differentiate first- and second-  
25 generation products. HOM monomers containing one to three N atoms (1-3N monomers) were formed, starting with  
26  $\text{NO}_3$  addition to carbon double bond, forming peroxy radicals ( $\text{RO}_2$ ), followed by autoxidation. 1N monomers were  
27 formed by both the direct reaction of  $\text{NO}_3$  with isoprene and of  $\text{NO}_3$  with first-generation products. 2N-monomers  
28 (e.g.  $\text{C}_5\text{H}_8\text{N}_2\text{O}_n$  ( $n=7-13$ ),  $\text{C}_5\text{H}_{10}\text{N}_2\text{O}_n$  ( $n=8-14$ )) were likely the termination products of  $\text{C}_5\text{H}_9\text{N}_2\text{O}_n\bullet$ , which was formed by  
29 the addition of  $\text{NO}_3$  to C5-hydroxynitrate ( $\text{C}_5\text{H}_9\text{NO}_4$ ), a first-generation product containing one carbon double bond.  
30 2N-monomers, which were second-generation products, dominated in monomers and accounted for ~34% of all  
31 HOM, indicating the important role of second-generation oxidation in HOM formation in the isoprene+ $\text{NO}_3$  reaction  
32 under our experimental conditions. H-shift of alkoxy radicals to form peroxy radicals and subsequent autoxidation  
33 (“alkoxy-peroxy” pathway) was found to be an important pathway of HOM formation. HOM dimers were mostly  
34 formed by the accretion reaction of various HOM monomer  $\text{RO}_2$  and via the termination reactions of dimer  $\text{RO}_2$   
35 formed by further reaction of closed-shell dimers with  $\text{NO}_3$  and possibly by the reaction of  $\text{C}_5\text{RO}_2$  with isoprene.  
36 HOM trimers were likely formed by the accretion reaction of dimer  $\text{RO}_2$  with monomer  $\text{RO}_2$ . The concentrations of  
37 different HOM showed distinct time profiles during the reaction, which was linked to their formation pathway. HOM  
38 concentrations either showed a typical time profile of first-generation products, or of second-generation products, or  
39 a combination of both, indicating multiple formation pathways and/or multiple isomers. Total HOM molar yield was  
40 estimated to be  $1.2\%^{+1.3\%}_{-0.7\%}$ , which corresponded to a SOA yield of ~3.6% assuming the molecular weight of  $\text{C}_5\text{H}_9\text{NO}_6$

41 as the lower limit. This yield suggests that HOM may contribute a significant fraction to SOA yield in the reaction  
42 of isoprene with  $\text{NO}_3$ .

43 **1 Introduction**

44 Highly oxygenated organic molecules (HOM) are an important class of compounds formed in the oxidation  
 45 of volatile organic compounds (VOC) including biogenic VOC (BVOC) and anthropogenic VOC (Crounse  
 46 et al., 2013; Ehn et al., 2014; Jokinen et al., 2014; Rissanen et al., 2014; Jokinen et al., 2015; Krechmer et al.,  
 47 2015; Mentel et al., 2015; Rissanen et al., 2015; Kenseth et al., 2018; Molteni et al., 2018; Garmash et al., 2019;  
 48 McFiggans et al., 2019; Molteni et al., 2019; Quelever et al., 2019). A number of recent studies have  
 49 demonstrated that HOM play a pivotal role in both nucleation and also particle growth of pre-existing particles,  
 50 thus contributing to secondary organic aerosol (SOA) (Ehn et al., 2014; Kirkby et al., 2016; Tröstl et al., 2016).  
 51 Particularly, in the early stage of aerosol growth, HOM may contribute a significant fraction of SOA mass  
 52 (Tröstl et al., 2016).

53 HOM are formed by the autoxidation of peroxy radicals ( $\text{RO}_2$ ), which means they undergo intramolecular  
 54 H-shift forming alky radicals, followed by  $\text{O}_2$  addition leading to formation of new  $\text{RO}_2$  as shown below  
 55 (Vereecken et al., 2007; Crounse et al., 2013; Ehn et al., 2017; Bianchi et al., 2019; Møller et al., 2019; Nozière  
 56 and Vereecken, 2019; Vereecken and Nozière, 2020).



57 Besides autoxidation, the  $\text{RO}_2$  can also react with  $\text{HO}_2$ ,  $\text{RO}_2$  and  $\text{NO}_3$ , either forming a series of termination  
 58 products (R1-3), including organic hydroperoxide, alcohol, and carbonyl, or forming alkoxy radicals ( $\text{RO}$ ,  
 59 R4-5) via the following reactions.



67 The termination products are detected in the mass spectra at masses M+1, M-15, M-17 respectively with  
 68 M being the molecular mass of the parent  $\text{RO}_2$  (Ehn et al., 2014; Mentel et al., 2015). In case that  $\text{RO}_2$  is an acyl  
 69 peroxy radical, percarboxylic acids and carboxylic acids are formed instead of hydroperoxides and alcohols in  
 70 R3 and R1, respectively (Atkinson et al., 2006; Mentel et al., 2015).  $\text{RO}_2$  can also form HOM dimers by the  
 71 accretion reaction of two  $\text{RO}_2$  (R6) (Berndt et al., 2018a; Berndt et al., 2018b; Valiev et al., 2019). Additionally,  
 72 HOM can be formed via H-shift in RO followed by  $\text{O}_2$  addition (referred to as “alkoxy-proxy” pathway)  
 73 (Finlayson-Pitts and Pitts, 2000; Vereecken and Peeters, 2010; Vereecken and Francisco, 2012; Mentel et al.,  
 74 2015). These pathways are summarized in a recent comprehensive review (Bianchi et al., 2019), which also  
 75 further clarifies HOM definition.

76 Currently, most laboratory studies of HOM formation focus on the VOC oxidation by OH and O<sub>3</sub> (Crounse  
77 et al., 2013; Ehn et al., 2014; Jokinen et al., 2014; Rissanen et al., 2014; Jokinen et al., 2015; Krechmer et al.,  
78 2015; Mentel et al., 2015; Rissanen et al., 2015; Kirkby et al., 2016; Tröstl et al., 2016; Kenseth et al., 2018;  
79 Molteni et al., 2018; Garmash et al., 2019; McFiggans et al., 2019; Molteni et al., 2019; Quelever et al., 2019;  
80 Wang et al., 2020; Yan et al., 2020). HOM formation in the oxidation of VOC with NO<sub>3</sub> has received much less  
81 attention. NO<sub>3</sub> is another important oxidant of VOC mainly operating during nighttime. Particularly, NO<sub>3</sub> has  
82 high reactivity with unsaturated BVOC such as monoterpane and isoprene. It is often the dominant oxidant of  
83 these compounds at night, especially in regions where biogenic and anthropogenic emissions mix (Geyer et al.,  
84 2001; Brown et al., 2009; Brown et al., 2011). The reaction products contribute to SOA formation (Xu et al.,  
85 2015; Lee et al., 2016). Also, the organic nitrates produced in these reactions play an important role in nitrogen  
86 chemistry by altering NO<sub>x</sub> concentration, which further influences photochemical recycling and ozone  
87 formation in the next day. Among these reaction products, HOM can also be formed (Xu et al., 2015; Lee et al.,  
88 2016; Yan et al., 2016). Despite the potential importance, studies of HOM formation in the oxidation of BVOC  
89 by NO<sub>3</sub> are still limited compared with the HOM formation via oxidation by O<sub>3</sub> and OH. Although a number of  
90 laboratory studies have investigated the reaction of NO<sub>3</sub> with BVOC (Ng et al., 2008; Fry et al., 2009; Rollins  
91 et al., 2009; Fry et al., 2011; Kwan et al., 2012; Fry et al., 2014; Boyd et al., 2015; Schwantes et al., 2015; Nah  
92 et al., 2016; Boyd et al., 2017; Claflin and Ziemann, 2018; Faxon et al., 2018; Draper et al., 2019; Takeuchi and  
93 Ng, 2019; Novelli et al., 2021; Vereecken et al., 2021), these studies mostly focus on either SOA yield and  
94 composition, or on the gas-phase chemistry mechanism mainly for “traditional” oxidation products that stem  
95 from few oxidation steps.

96 Importantly, HOM formation in the reaction of NO<sub>3</sub> with isoprene, the most abundant BVOC accounting  
97 for more than half of the global BVOC emissions, has not been explicitly addressed yet, to the best of our  
98 knowledge. Although isoprene from plants are mainly emitted under light conditions, i.e., in the daytime,  
99 isoprene can remain high after sunset in significant concentrations (Starn et al., 1998; Stroud et al., 2002; Brown et  
100 al., 2009) because of the reduced consumption by OH and is found to decay rapidly. A substantial fraction of  
101 isoprene can then be oxidized by NO<sub>3</sub> (Brown et al., 2009). Regarding the budget of NO<sub>3</sub>, the reaction of isoprene  
102 with NO<sub>3</sub> can contribute to a significant or even dominant fraction of NO<sub>3</sub> loss at night in regions where VOC is  
103 dominated by isoprene such as Northeast US (Brown et al., 2009). Under some circumstances, the reaction of isoprene  
104 with NO<sub>3</sub> can contribute to a significant fraction during the afternoon and afterwards (Ayres et al., 2015; Hamilton  
105 et al., 2021). The reaction of isoprene with NO<sub>3</sub> is the subject of a number of studies (Ng et al., 2008; Perring et  
106 al., 2009; Rollins et al., 2009; Kwan et al., 2012; Schwantes et al., 2015; Vereecken et al., 2021). These studies  
107 focus on the oxidation mechanism and “traditional” oxidation products, as well as SOA yields. The initial step  
108 is the NO<sub>3</sub> addition to one of the C=C double bounds, preferentially to the carbon C1 (Schwantes et al., 2015),  
109 followed by O<sub>2</sub> addition forming a nitrooxyalkyl peroxy radical (RO<sub>2</sub>). This RO<sub>2</sub> can undergo the reactions  
110 described above, forming a series of products such as C5-nitrooxyhydroperoxide, C5-nitrooxycarbonyl, and C5-  
111 hydroxynitrate (Ng et al., 2008; Kwan et al., 2012), as well as methyl vinyl ketone (MVK), potentially  
112 methacrolein (MACR), formaldehyde, OH radical, and NO<sub>2</sub> as minor products (Schwantes et al., 2015). A high

113 nitrate yield (57-95%) was found (Perring et al., 2009; Rollins et al., 2009; Kwan et al., 2012; Schwantes et al.,  
114 2015). Products in the particle phase such as C<sub>10</sub> dimers were also detected (Ng et al., 2008; Kwan et al., 2012;  
115 Schwantes et al., 2015). The SOA yield varies from 2% to 23.8% depending on the organic aerosol concentration  
116 (Ng et al., 2008; Rollins et al., 2009). These studies have provided valuable insights in oxidation mechanism,  
117 particle yield and composition. However, because HOM formation was not the focus of these studies, only a  
118 limited number of products, mainly moderately oxygenated ones (oxygen number  $\leq 2$  in addition to NO<sub>3</sub>  
119 functional groups), were detected in the gas phase. The detailed mechanism of HOM formation and their yields  
120 in the reaction of BVOC+NO<sub>3</sub> are still unclear.

121 In this study, we investigated the HOM formation in the oxidation of isoprene by NO<sub>3</sub>. We report the  
122 identification of HOM, including HOM monomers, dimers, and trimers. According to the reaction products and  
123 literature, we discuss the formation mechanism of these HOM. The formation mechanism of various HOM is  
124 further constrained with time series of HOM upon repeated isoprene additions. We also provide an estimate of  
125 HOM yield in the isoprene+NO<sub>3</sub> reaction and assess their roles in SOA formation.

## 126 2 Experimental

### 127 2.1 Chamber setup and experiments

128 Experiments investigating the reaction of isoprene with NO<sub>3</sub> were conducted in the SAPHIR chamber  
129 (Simulation of Atmospheric PHotochemistry In a large Reaction chamber) at Forschungszentrum Jülich,  
130 Germany. The details of the chamber have been described before (Rohrer et al., 2005; Zhao et al., 2015a; Zhao  
131 et al., 2015b; Zhao et al., 2018). Briefly, SAPHIR is a Teflon chamber with a volume of 270 m<sup>3</sup>. It can utilize  
132 natural sunlight for illumination and is equipped with a louvre system to switch between light and dark  
133 conditions. In this study, the experiments were conducted in the dark with the louvres closed.

134 Temperature and relative humidity were continuously measured. Gas and particle phase species were  
135 characterized using a comprehensive set of instruments with the details described before (Zhao et al., 2015b).  
136 VOC were characterized using a Proton Transfer Reaction Time-of-Flight Mass Spectrometer (PTR-ToF-MS,  
137 Ionicon Analytik, Austria). NO<sub>x</sub> and O<sub>3</sub> concentrations were measured using a chemiluminescence NO<sub>x</sub> analyzer  
138 (ECO PHYSICS TR480) and an UV photometer O<sub>3</sub> analyzer (ANSYCO, model O341M), respectively. OH,  
139 HO<sub>2</sub> and RO<sub>2</sub> concentrations were measured using a laser induced fluorescence system (LIF) (Fuchs et al., 2012).  
140 NO<sub>3</sub> and N<sub>2</sub>O<sub>5</sub> were detected by a custom-built instrument based on cavity ring-down spectroscopy. The design  
141 of the instrument is similar to that described by Wagner et al. (2011). NO<sub>3</sub> was directly detected in one cavity  
142 by its absorption at 662 nm and the sum of NO<sub>3</sub> and N<sub>2</sub>O<sub>5</sub> in a second, heated cavity, which had a heated inlet  
143 to thermally decompose N<sub>2</sub>O<sub>5</sub> to NO<sub>3</sub>. The sampling flow rate was 3 to 4 liters per minute. The detection by  
144 cavity ring-down spectroscopy was achieved by a diode laser that was periodically switched on and off with a  
145 repetition rate of 200 Hz. Ring-down events were observed by a digital oscilloscope PC card during the time  
146 when the laser was switched off and were averaged over 1s. The zero-decay time that is needed to calculate the  
147 concentration of NO<sub>3</sub> was measured every 20 s by chemically removing NO<sub>3</sub> in the reaction with excess nitric

148 oxide (NO) in the inlet system. The accuracy of measurements was limited by the uncertainty in the correction  
149 for inlet losses of NO<sub>3</sub> and N<sub>2</sub>O<sub>5</sub>. In the case of N<sub>2</sub>O<sub>5</sub> a transmission of (85±10) % was achieved and in the case  
150 of NO<sub>3</sub> of (50±30) %.

151 Before an experiment, the chamber was flushed with high purity synthetic air (purity>99.9999% O<sub>2</sub> and N<sub>2</sub>).  
152 Experiments were conducted under dry condition (RH<2 %) and temperature was at 302±3 K. NO<sub>2</sub> and O<sub>3</sub> were  
153 added to the chamber first to form N<sub>2</sub>O<sub>5</sub> and NO<sub>3</sub>, reaching concentrations of ~60 ppb for NO<sub>2</sub> and ~100 ppb for O<sub>3</sub>.  
154 After around half an hour, isoprene was sequentially added into the chamber for three times at intervals of ~1 h.  
155 Around 40 min after the third isoprene injection, NO<sub>2</sub> was added to compensate the loss of NO<sub>3</sub> and N<sub>2</sub>O<sub>5</sub>. Afterwards,  
156 three isoprene additions were repeated in the same way as before. O<sub>3</sub> was added before the fifth and the sixth isoprene  
157 addition to compensate for its loss by reaction. The schematic for the experimental procedure is shown in Fig. S1.  
158 Experiments were designed such that the chemical system was dominated by the reaction of isoprene with NO<sub>3</sub> and  
159 the reaction of isoprene with O<sub>3</sub> did not play a major role (<3% of the isoprene consumption). Figure S2 shows the  
160 relative contributions of the reaction of O<sub>3</sub> and NO<sub>3</sub> with isoprene to the total chemical loss of isoprene using the  
161 NO<sub>3</sub> and O<sub>3</sub> concentrations measured. The reaction with NO<sub>3</sub> accounted for >95% of the isoprene consumption for  
162 the whole experiments. The contribution of the reaction of isoprene with trace amount of OH, mainly produced in  
163 the reaction of isoprene+O<sub>3</sub> via Criegee intermediates (Nguyen et al., 2016), is negligible as the OH yield is less than  
164 one (Malkin et al., 2010) and thus its contribution is less than that of isoprene+O<sub>3</sub>. This is consistent with the  
165 contribution determined using measured OH concentration, despite some uncertainty in measured OH concentration  
166 due to the interference from NO<sub>3</sub>. In these experiments, RO<sub>2</sub> fate is estimated to be dominated by its reaction with  
167 NO<sub>3</sub> according to the measured NO<sub>3</sub>, RO<sub>2</sub>, and HO<sub>2</sub> concentration and their rate constants for the reactions with RO<sub>2</sub>  
168 (MCM v3.2(Jenkin et al., 1997; Jenkin et al., 2003; Saunders et al., 2003; Jenkin et al., 2015), via website:  
169 <http://mcm.leeds.ac.uk/MCM>) despite uncertainties of the measured RO<sub>2</sub> and HO<sub>2</sub> concentration due to interference  
170 from NO<sub>3</sub>. As a large portion of RO<sub>2</sub> is not measured by LIF (Vereecken et al., 2021) and thus RO<sub>2</sub> is underestimated,  
171 we expected the reaction of RO<sub>2</sub>+RO<sub>2</sub> to be also important. Overall, we estimate that the RO<sub>2</sub> fate is dominated by  
172 the reaction RO<sub>2</sub>+NO<sub>3</sub> with significant contribution of RO<sub>2</sub>+RO<sub>2</sub>.

## 173 2.2 Characterization of HOM

174 In this study we refer to similar definition for HOM by Bianchi et al. (2019), i.e., HOM typically contain six or  
175 more oxygen atoms formed via autoxidation and related chemistry of peroxy radicals. HOM were detected using a  
176 Chemical Ionization time-of-flight Mass Spectrometer (Aerodyne Research Inc., USA) with nitrate as the reagent ion  
177 (CIMS) (Eisele and Tanner, 1993; Jokinen et al., 2012). <sup>15</sup>N nitric acid was used to produce <sup>15</sup>NO<sub>3</sub><sup>-</sup> in order to  
178 distinguish the NO<sub>3</sub> group in target molecules formed in the reaction from the reagent ion. The details of the  
179 instrument are described in our previous publications (Ehn et al., 2014; Mentel et al., 2015; Pullinen et al., 2020).  
180 The CIMS has a mass resolution of ~4000 (m/dm). Examples of peak fitting are shown in Fig. S3. HOM  
181 concentrations were estimated using the calibration coefficient of H<sub>2</sub>SO<sub>4</sub> as described by Pullinen et al. (2020)  
182 because the charge efficiency of HOM and H<sub>2</sub>SO<sub>4</sub> can be assumed to be equal and close to the collision limit (Ehn et  
183 al., 2014; Pullinen et al., 2020). The details of the calibration with H<sub>2</sub>SO<sub>4</sub> are provided in the supplement S1. Since  
184 HOM contain more than six oxygen atoms and their clusters with nitrate ions are quite stable (Ehn et al., 2014), the

185 charge efficiency of HOM is thus assumed to be equal to that of  $\text{H}_2\text{SO}_4$ , which is close to the collision limit (Viggiano  
186 et al., 1997). If HOM do not charge with nitrate ions at their collision limit or the clusters formed break during the  
187 short residence time in the charger, its concentration would be underestimated as pointed by Ehn et al. (2014). Thus,  
188 our assumption provides a lower limit of the HOM concentration. The HOM yield was derived using the  
189 concentration of the HOM produced, divided by the concentration of isoprene that was consumed by  $\text{NO}_3$ . The  
190 uncertainty of HOM yield was estimated to  $-55\% / +103\%$ . The loss of HOM to the chamber was corrected using a  
191 wall loss rate of  $6 \times 10^{-4} \text{ s}^{-1}$  as quantified previously (Zhao et al., 2018). HOM concentrations were also corrected for  
192 dilution due to the replenishment flow needed to maintain a constant overpressure of the chamber (loss rate  $\sim 1 \times 10^{-6}$   
193  $\text{s}^{-1}$ ) (Zhao et al., 2015b). The influence of wall loss correction and dilution correction on HOM yield was  $\sim 12\%$  and  
194  $<1\%$ , respectively. Although the wall loss rate of vapors in this study might not be exactly the same as in our previous  
195 photo-oxidation experiments (Zhao et al., 2018), HOM yield is not sensitive to the vapor wall loss rate. An increase  
196 of wall loss rate by 100% or a decrease by 50% only changes the HOM yield by 11% and -6%, respectively.

### 197 3 Results and discussion

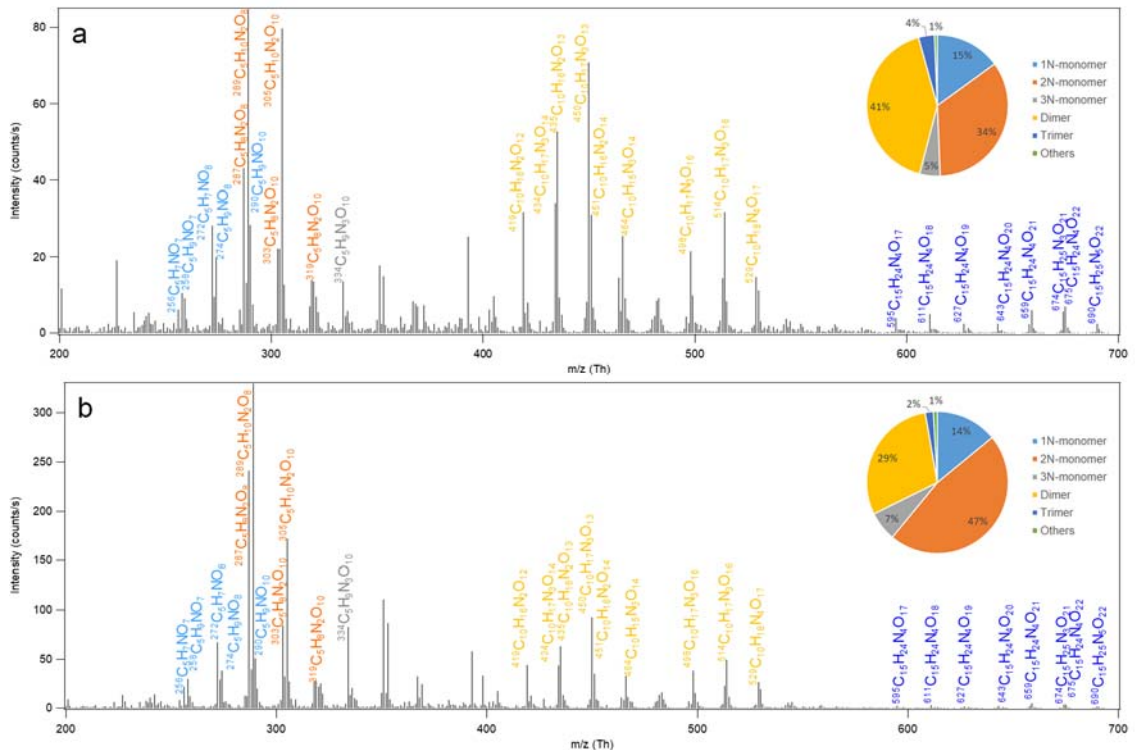
#### 198 3.1 Overview of HOM

199 The mass spectra of HOM in the gas phase formed in the oxidation of isoprene by  $\text{NO}_3$  are shown in  
200 Fig. 1. A large number of HOM were detected. Almost all peaks are assigned HOM containing nitrogen atoms  
201 with possibly few exceptions such as  $\text{C}_5\text{H}_{10}\text{O}_8$  and  $\text{C}_5\text{H}_8\text{O}_{11}$  with very minor peaks ( $\sim 1\%$  of the maximum  
202 peak). The reaction products can be roughly divided into three classes: monomers (C5,  $\sim 200$ -400 Th), dimers  
203 (C10,  $\sim 400$ -600 Th), and trimers (C15,  $\sim 600$  Th), according to their mass to charge ratio ( $\text{m/z}$ ). The detailed  
204 peak assignment of monomers, dimers, and trimers is discussed in the following sections.

#### 205 3.2 HOM monomers and their formation

##### 206 3.2.1 Overview of HOM monomers

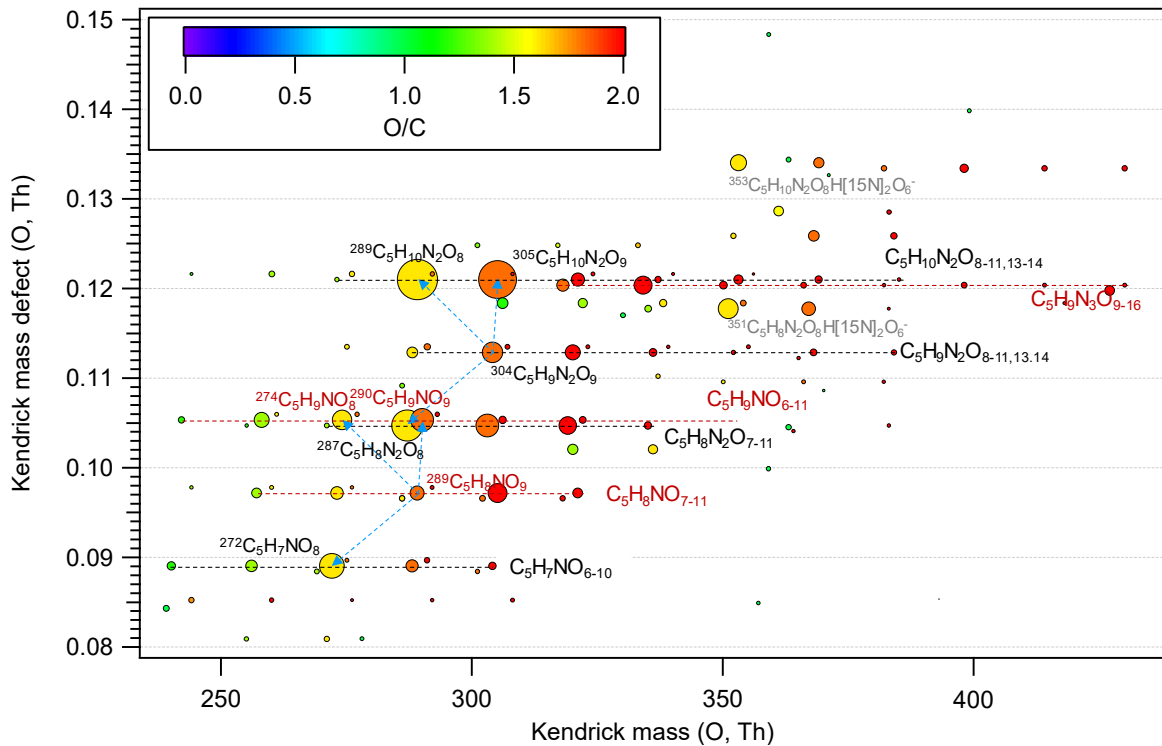
207 HOM monomers showed a roughly repeating pattern in the mass spectrum at every 16 Th  
208 (corresponding to the mass of oxygen) (Fig. 1a). Here a number of series of HOM monomers with continuously  
209 increasing oxygenation were found, such as  $\text{C}_5\text{H}_9\text{NO}_n$ ,  $\text{C}_5\text{H}_7\text{NO}_n$ ,  $\text{C}_5\text{H}_8\text{N}_2\text{O}_n$ ,  $\text{C}_5\text{H}_{10}\text{N}_2\text{O}_n$  (Table 1, Table S1-2  
210 and Fig. 2). These monomers included both stable closed-shell molecules and open-shell radicals, such as  
211  $\text{C}_5\text{H}_8\text{NO}_n\bullet$  and  $\text{C}_5\text{H}_9\text{N}_2\text{O}_n\bullet$ . The open-shell molecules were likely  $\text{RO}_2$  radicals because of their much longer life  
212 time and hence higher concentrations compared with alkoxy radicals (RO) and alkyl radicals (R). Since the  
213 observed stable products were mostly termination products of  $\text{RO}_2$  reactions, we describe the stable products in  
214 a  $\text{RO}_2$ -oriented approach. It is worth noting that some of the termination products may contain multiple isomers  
215 formed from different pathways.



216 Figure 1. Mass spectrum of the HOM formed in the oxidation of isoprene by  $\text{NO}_3^-$ . HOM are detected as

217 clusters with the reagent ion  $^{15}\text{NO}_3^-$ , which is not shown in the molecular formula in the figure for simplicity. Panel  
 218 a and b show the average spectrum during the first isoprene addition period (P1) and for the whole period of six  
 219 isoprene additions (P1-6), respectively. The insets show the contributions of different classes of HOM. 1-3N-  
 220 monomer refers to the monomers containing 1-3 nitrogen atoms in the molecular formula.

221 HOM monomers were classified into 1N-, 2N-, and 3N-monomers according to the number of nitrogen  
 222 atoms that they contain. HOM without nitrogen atoms were barely observed except for very minor peaks ( $\sim 1\%$  of  
 223 the maximum peak) possibly assigned to  $\text{C}_5\text{H}_{10}\text{O}_8$  and  $\text{C}_5\text{H}_8\text{O}_{11}$ . The contribution of 2N-monomers such as  
 224  $\text{C}_5\text{H}_{10}\text{N}_2\text{O}_n$  and  $\text{C}_5\text{H}_8\text{N}_2\text{O}_n$  was higher than that of the 1N-HOM monomers, and that of 3N-monomers was the least  
 225 (Fig. 1, inset). The most abundant monomers were  $\text{C}_5\text{H}_{10}\text{N}_2\text{O}_8$ ,  $\text{C}_5\text{H}_{10}\text{N}_2\text{O}_9$ , and  $\text{C}_5\text{H}_8\text{N}_2\text{O}_8$ . The termination products  
 226 of  $\text{C}_5\text{H}_9\text{NO}_8$ ,  $\text{C}_5\text{H}_9\text{NO}_9$ , and  $\text{C}_5\text{H}_7\text{NO}_8$  also showed relatively high abundance. These limited number of compounds  
 227 dominated the HOM monomers. Since 2N-monomers were second-generation products as discussed below, the  
 228 higher abundance 2N- monomers indicate that the second-generation HOM play an important role in the reaction of  
 229  $\text{NO}_3^-$  with isoprene in the reaction conditions of our study, as also seen by Wu et al. (2020) . This is more evident for  
 230 the mass spectrum averaged over six isoprene addition periods (Fig. 1b), where the abundance of  $\text{C}_5\text{H}_{10}\text{N}_2\text{O}_n$  and  
 231  $\text{C}_5\text{H}_8\text{N}_2\text{O}_n$  were more dominant. This observation is in contrast with the finding for the reaction of  $\text{O}_3$  with BVOC  
 232 which contains only one double bond such as  $\alpha$ -pinene (Ehn et al., 2014), where HOM are mainly first-generation  
 233 products formed via autoxidation. The higher abundance of HOM 2N-monomers than 1N-monomers is likely because  
 234 HOM production rate via the autoxidation of 1N-monomer  $\text{RO}_2$  following the reaction of isoprene with  $\text{NO}_3^-$  may be  
 235 slower than that of the reaction of 1N-monomers (including both HOM and non-HOM monomers) with  $\text{NO}_3^-$ . We  
 236 would like to note that some less oxygenated 1N-monomers such as  $\text{C}_5\text{H}_9\text{NO}_{4/5}$  and  $\text{C}_5\text{H}_7\text{NO}_4$  may have high  
 237 abundance but are not detected by  $\text{NO}_3^-$ -CIMS and are not HOM and thus not included in HOM 1N-monomers.



239

240

Figure 2. Kendrick mass defect plot for O of HOM monomers. The m/z in the molecular formula include the reagent ion  $^{15}\text{NO}_3^-$ , which is not shown for simplicity. The size (area) of circles is set to be proportional to the average peak intensity of each molecular formula during the first isoprene addition period (P1). The species at m/z 351 and 353 (labelled in grey) are the adducts of  $\text{C}_5\text{H}_8\text{N}_2\text{O}_8$  and  $\text{C}_5\text{H}_{10}\text{N}_2\text{O}_8$  with  $\text{H}[15\text{N}]_2\text{O}_6^-$ , respectively. The blue dashed lines with arrows indicate the termination product hydroperoxide ( $\text{M}+\text{H}$ ), alcohol ( $\text{M}-\text{O}+\text{H}$ ), and ketone ( $\text{M}-\text{O}-\text{H}$ ) with  $\text{M}$  the molecular formula of a HOM  $\text{RO}_2$ .

### 246 3.2.2 1N-monomers

247 In our experiments we observed a  $\text{C}_5\text{H}_8\text{NO}_n\bullet$  ( $n=7-12$ ) series (series M1), as well as its corresponding 248 termination products  $\text{C}_5\text{H}_7\text{NO}_{n-1}$ ,  $\text{C}_5\text{H}_9\text{NO}_{n-1}$ , and  $\text{C}_5\text{H}_9\text{NO}_n$  via the reactions with  $\text{RO}_2$  and  $\text{HO}_2$ , which contain 249 carbonyl, hydroxyl, and hydroperoxy group, respectively. Overall, the peak intensities of  $\text{C}_5\text{H}_9\text{NO}_n$  and 250  $\text{C}_5\text{H}_7\text{NO}_n$  series first increased and then decreased as oxygen number increased (Fig. 2), with the peak intensity 251 of  $\text{C}_5\text{H}_9\text{NO}_8$  and  $\text{C}_5\text{H}_7\text{NO}_8$  being the highest within their respective series when averaged over the whole 252 experiment period.

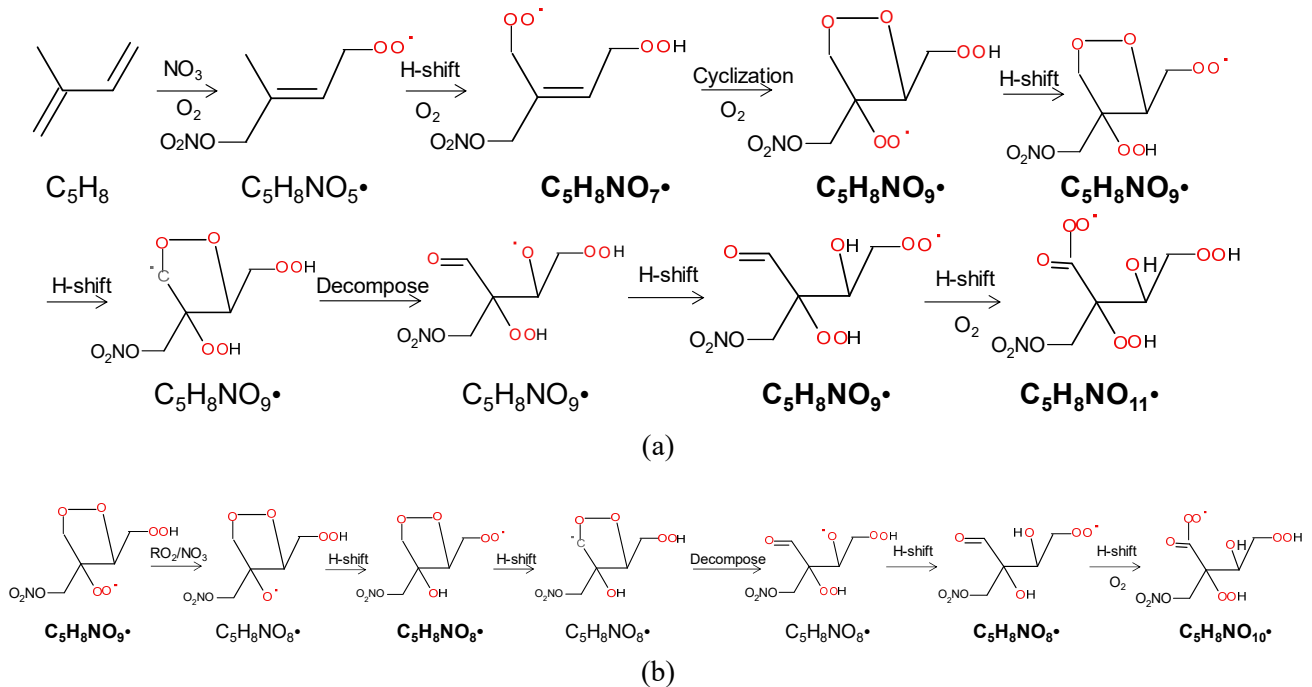
253 Table 1. HOM monomers formed in the oxidation of isoprene by  $\text{NO}_3$ .

Series Number	Product	Type <sup>a</sup>	Pathway of $\text{RO}_2$
M1a/b	$\text{C}_5\text{H}_8\text{NO}_n$ ( $n=7-11$ )	$\text{RO}_2$	
	$\text{C}_5\text{H}_9\text{NO}_n$ ( $n=6-11$ )	$\text{ROOH/ROH}$	$\text{Isoprene}+\text{NO}_3$
	$\text{C}_5\text{H}_7\text{NO}_n$ ( $n=6-10$ )	$\text{R=O}$	$\text{Isoprene}+\text{NO}_3+\text{NO}_3$
M2a/b	$\text{C}_5\text{H}_9\text{N}_2\text{O}_n$ ( $n=8-11,13,14$ ) <sup>b</sup>	$\text{RO}_2$	
	$\text{C}_5\text{H}_{10}\text{N}_2\text{O}_n$ ( $n=8-11,13,14$ ) <sup>b</sup>	$\text{ROOH/ROH}$	$\text{Isoprene}+\text{NO}_3+\text{NO}_3$
	$\text{C}_5\text{H}_8\text{N}_2\text{O}_n$ ( $n=7-11$ )	$\text{R=O}$	

	$C_5H_9N_3O_n$ (n=9-16) <sup>b</sup>	$RO_2NO_2$	
M3	$C_5H_7N_2O_{n(n=9)}$	$RO_2$	
	$C_5H_8N_2O_{n(n=8, 9)}$	$ROOH/ROH$	Isoprene + $NO_3 + NO_3$
	$C_5H_6N_2O_{n(n=8)}$	$R=O$	
M4	$C_5H_{10}NO_{n(n=8-9)}$	$RO_2$	
	$C_5H_{11}NO_{n(n=7-9)}$	$ROOH/ROH$	Isoprene + $NO_3 + OH$
	$C_5H_9NO_{n(n=7-8)}$	$R=O$	

254 <sup>a</sup>:  $RO_2$  denotes peroxy radical and  $ROOH$ ,  $ROH$ ,  $R=O$ , and  $RO_2NO_2$  denote the termination products  
 255 containing hydroperoxy, hydroxyl, carbonyl group, and peroxy nitrate, respectively.

256 <sup>b</sup>: Peak assignment of compounds with n=13,14 may be subject to uncertainties.



270 Scheme 1. The example pathways to form HOM  $RO_2 C_5H_8NO_n\cdot$  (n=7, 9, 11) series (a) and  $C_5H_8NO_n\cdot$   
 271 (n=8, 10) series (b) in the reaction of isoprene with  $NO_3$ . The detected products are in bold.

272  $C_5H_8NO_n\cdot$  with odd number oxygen atoms (n=7, 9, 11, series M1a) were possibly formed by the attack  
 273 of  $NO_3$  to one double bond (preferentially to C1 according to previous studies (Skov et al., 1992; Berndt and  
 274 Böge, 1997; Schwantes et al., 2015) and followed by autoxidation (Scheme 1a). We would like to note that  
 275  $NO_3^-$ -CIMS only observed HOM with oxygen numbers  $\geq 6$  in this study due to its selectivity of detection.  
 276  $C_5H_8NO_n\cdot$  with even number oxygen atoms (n=8, 10, series M1b in Table 1) were possibly formed after H-shift  
 277 of an alkoxy radical formed in reaction R4 or R5 and subsequent  $O_2$  addition (“alkoxy-peroxy” channel)  
 278 (Scheme 1b), where the alkoxy radicals can be formed both from the  $RO_2+NO_3$  and  $RO_2+RO_2$  reactions. The  
 279 hydroxy $RO_2$  formed can undergo further autoxidation adding two oxygen atoms after each H-shift. We would  
 280 like to note that the scheme and other schemes in this study only show example isomers and pathways to form these

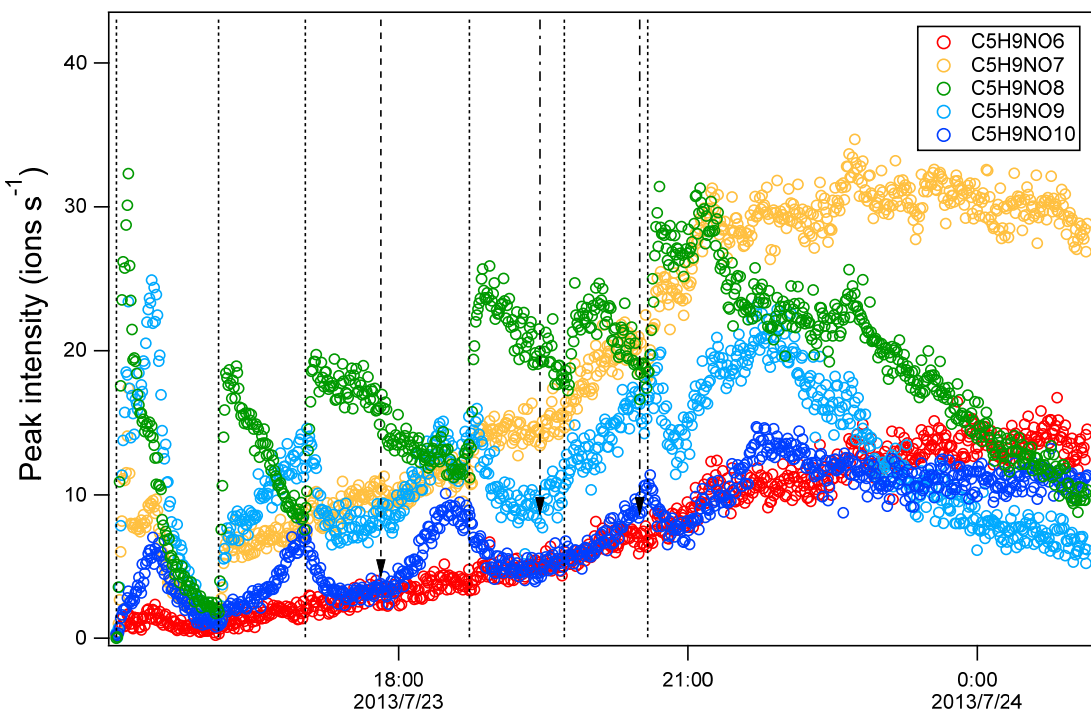
273 molecules. It is likely that many of the reactions occurring are not the dominant channels as otherwise there would  
274 be much higher HOM yield as discussed below.

275 Some HOM monomers may contain multiple isomers and be formed via different pathways. For  
276 example,  $C_5H_9NO_n$  can contain alcohols derived from  $RO_2 C_5H_8NO_{n+1}\bullet$ , hydroperoxides derived from  $RO_2$   
277  $C_5H_8NO_n\bullet$  or the ketones from  $RO_2 C_5H_{10}NO_{n+1}\bullet$ . Some  $RO_2 C_5H_8NO_n\bullet$  may be formed via the reaction of first-  
278 generation products with  $NO_3$  in addition to direct reaction of isoprene with  $NO_3$ . For example,  $C_5H_8NO_7\bullet$  can  
279 be formed by the reaction of  $NO_3$  with  $C_5H_8O_2$ , which is a first-generation product observed previously in the  
280 reaction of isoprene with  $NO_3$  or OH (Scheme S1b) (Kwan et al., 2012). Moreover,  $RO_2 C_5H_8NO_n\bullet$  can be  
281 formed from C5-carbonylnitrate, a first-generation product, with OH (Scheme S1a). Trace amount of OH can  
282 be produced in the reaction of isoprene with  $NO_3$  (Kwan et al., 2012; Wennberg et al., 2018). OH can also be  
283 formed via Criegee intermediates formed in the isoprene+ $O_3$  reaction (Nguyen et al., 2016), but this OH source  
284 was likely minor because the contribution of the isoprene+ $O_3$  reaction to total isoprene loss was negligible (<5%,  
285 Fig. S2). In addition,  $C_5H_8NO_8\bullet$  may also be formed by the reaction of  $NO_3$  with  $C_5H_8O_3$ , which is a first-  
286 generation product observed in the reaction of isoprene with OH (Kwan et al., 2012). The  $C_5H_8NO_n\bullet$  formed  
287 via direct reaction of isoprene with  $NO_3$  is a first-generation  $RO_2$  while that formed via other indirect pathways  
288 is a second-generation  $RO_2$ . The time profile of the isomers from these two pathways, however, are expected to  
289 be different as will be discussed below.

290 Time series of HOM can shed light on their formation mechanisms. It is expected that first-generation  
291 products increase fast with isoprene addition and reach a maximum earlier in the presence of wall loss of organic  
292 vapour, while second-generation products reach a maximum in the later stage or increase continuously if the  
293 production rate is higher than the loss rate. As a reference to analyze the time profiles of HOM, the times profile  
294 of isoprene,  $NO_3$ , and  $N_2O_5$  are also shown (Fig. S4). After isoprene was added in each period,  $NO_3$  and  $N_2O_5$   
295 dropped dramatically and then gradually increased. We found that termination products within the same M1  
296 series showed different time profiles. For example, in  $C_5H_9NO_n$  series,  $C_5H_9NO_8$  clearly increased  
297 instantaneously with isoprene addition, and decreased fast afterwards (Fig. 3a), indicating that it was a first-  
298 generation product, which was expected according to the mechanism Scheme 1.  $C_5H_9NO_6$  and  $C_5H_9NO_{10}$  had a  
299 general increasing trend with time. While  $C_5H_9NO_6$  increased continuously with time,  $C_5H_9NO_{10}$  reached  
300 maximum intensity in the late phase of each isoprene addition period and then decreased naturally or after  
301 isoprene addition. The faster loss of  $C_5H_9NO_{10}$  than  $C_5H_9NO_6$  may result from the faster wall loss due to its  
302 lower volatility.  $C_5H_9NO_7$  and  $C_5H_9NO_9$  showed a mixing time profile with features of the former two kinds of  
303 time profiles, increasing almost instantaneously with isoprene additions, especially in the first two periods,  
304 while increasing continuously or decreasing first with isoprene additions and then increasing later in each period.  
305 This kind of time series indicates that there were significant contributions from both first- and second-generation  
306 products.

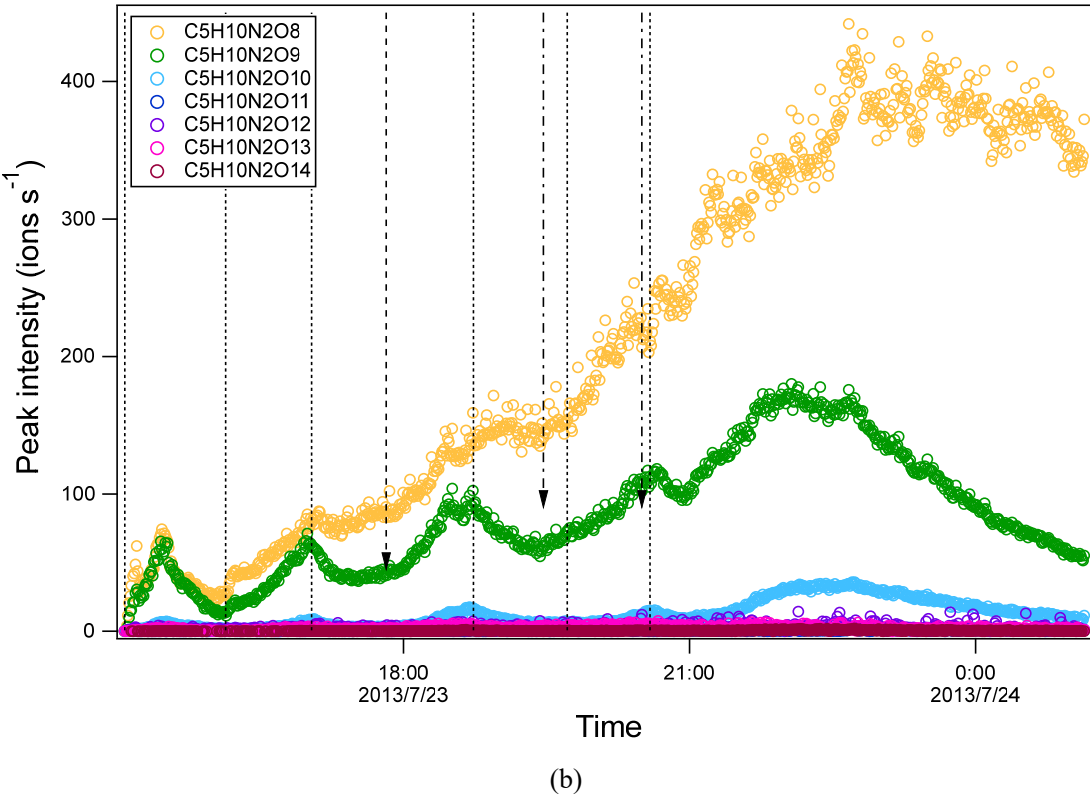
307 The second-generation products may be different isomers formed in pathways other than shown in  
308 Scheme 1. Second-generation  $C_5H_9NO_6$  can be formed via  $C_5H_8NO_7\bullet$ , which can also be formed by the reaction  
309 of  $NO_3$  and  $O_2$  with  $C_5H_8O_2$  as mentioned above (Scheme S2b), or by the reaction of OH with  $C_5H_7NO_4$  (Scheme

310 S2a). The time profiles of  $C_5H_8NO_7\bullet$  did show more contribution of second-generation processes because it  
 311 continuously increased with time in general. If the pathways via the reaction of  $NO_3$  and  $O_2$  with  $C_5H_8O_2$  and  
 312 the reaction of OH with  $C_5H_7NO_4$  contribute most to  $C_5H_9NO_6$ ,  $C_5H_9NO_6$  would show mostly a time profile of  
 313 second-generation products. Similarly, second-generation  $C_5H_9NO_7$  can be formed via  $C_5H_8NO_7\bullet$  or  $C_5H_8NO_8\bullet$ .  
 314 The time series of  $C_5H_8NO_8\bullet$  did show the contribution of both the first- and second-generation processes, which  
 315 generally increased with time while also responding to isoprene addition (Fig. S5). Similar to  $C_5H_9NO_6$ , the  
 316 second-generation pathway for  $C_5H_9NO_7$ ,  $C_5H_9NO_9$ , and  $C_5H_9NO_{10}$  are shown in Scheme S1, S3, S4. For the  
 317  $RO_2$  in  $C_5H_8NO_n\bullet$  series other than  $C_5H_8NO_{7/8}\bullet$ , the peak of  $C_5H_8NO_n\bullet$  overlaps with  $C_5H_{10}N_2O_n$  in the mass  
 318 spectra, which is a much larger peak, and thus cannot be differentiated from  $C_5H_{10}N_2O_n$ . Therefore, it is not  
 319 possible to obtain reliable separate time profiles in order to differentiate their major sources. It is worth noting  
 320 that nitrate CIMS may not be able to detect all isomers of  $C_5H_9NO_6$  due to the sensitivity limitation. Therefore,  
 321 we cannot exclude the possibility that the absence of some first-generation isomers of  $C_5H_9NO_6$  was due to the  
 322 low sensitivity of these isomers.



(a)

323  
 324



325  
326

(b)

327       Figure 3. Time series of peak intensity of several HOM monomers of  $C_5H_9NO_n$  series (a) and of  $C_5H_{10}N_2O_n$  series (b). They are likely the termination products of  $RO_2$   $C_5H_8NO_n\cdot$  and  $C_5H_9N_2O_n\cdot$ , respectively. The dashed lines  
328 indicate the time of isoprene additions. The long-dashed arrow indicates the time of  $NO_2$  addition. The dash-dotted  
329 arrows indicate the time of  $O_3$  additions.  
330

331       Among the termination products of the 1N-monomer  $RO_2$ , carbonyl and hydroxyl/hydroperoxide  
332 species had comparable abundance in general (Table S1), suggesting that disproportionation reactions between  
333  $RO_2$  and  $RO_2$  forming hydroxy and carbonyl species (R1-2) was likely an important  $RO_2$  termination pathway.  
334 However, dependence of the exact ratio of carbonyl species to hydroxyl/hydroperoxide species on the number  
335 of oxygen atoms did not show a clear trend (Table S1), suggesting that the reactions of HOM  $RO_2$  depended on  
336 their specific structure. There was no clear difference in the abundance between the termination products from  
337  $C_5H_8NO_n\cdot$  with odd and even number of oxygen atom in general, although the most abundant termination  
338 product of  $C_5H_8NO_n\cdot$ , i.e.  $C_5H_7NO_8$ , was likely formed from  $C_5H_8NO_9\cdot$  in series M1a. This fact indicates that  
339 both the peroxy pathway and alkoxy-peroxy pathway were important for the HOM formation in the  
340 isoprene+ $NO_3$  reaction under our conditions, in agreement with the significant formation of alkoxy radicals  
341 from the reaction of  $RO_2$  with  $NO_3$  and  $RO_2$ .

342       In addition to the termination products of  $RO_2$  M1, minor peaks of the  $RO_2$  series  $C_5H_{10}NO_n\cdot$  ( $n=8-9$ ) (M4,  
343 Table 1) and their corresponding termination products including hydroperoxide, alcohol and carbonyl species were  
344 detected (Table S3).  $C_5H_{10}NO_n$  were likely formed by sequential addition of  $NO_3$  and  $OH$  to two double bonds of  
345 isoprene (Scheme S5).  $OH$  can react fast with isoprene or with the first-generation products of the reaction of isoprene

346 with  $\text{NO}_3$ , thus forming  $\text{C}_5\text{H}_{10}\text{NO}_{n\bullet}$ . In addition, a few very minor but noticeable peaks of  $\text{C}_5\text{H}_9\text{O}_{n\bullet}$  and their  
347 corresponding termination products  $\text{C}_5\text{H}_{10}\text{O}_n$  and  $\text{C}_5\text{H}_8\text{O}_n$  were also observed. These HOM may be formed by the  
348 reactions of isoprene with trace amount of OH and with  $\text{O}_3$ , although their contributions to reacted isoprene were  
349 negligible. These HOM were also observed in the reaction of isoprene with  $\text{O}_3$  with and without OH scavengers  
350 (Jokinen et al., 2015).

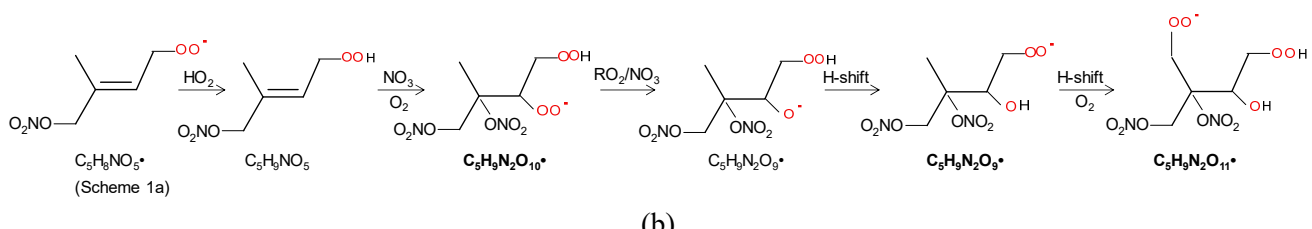
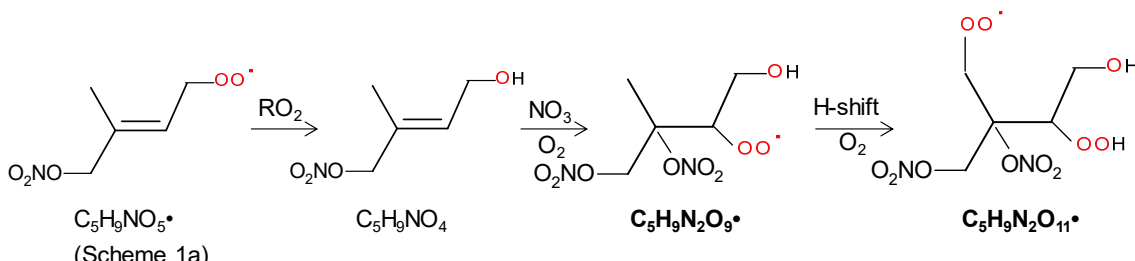
351 Among 1N-monomer HOM,  $\text{C}_5\text{H}_9\text{NO}_7$  has been observed in the particle phase using ESI-TOFMS by  
352 Ng et al. (2008) while others have not been observed in previous laboratory studies of the reaction of isoprene  
353 with  $\text{NO}_3$ , to our knowledge. A number of  $\text{C}_5$  organic nitrates have been observed in field studies. For example,  
354  $\text{C}_5\text{H}_{7-11}\text{NO}_{6-8}$  and  $\text{C}_5\text{H}_{7-11}\text{NO}_{4-9}$  have been observed in the gas phase (Massoli et al., 2018) and -the aerosol  
355 particle phase (Lee et al., 2016; Chen et al., 2020) ~~s, respectively during the Southern Oxidant and Aerosol Study~~  
356 in a rural area~~Alabama, of southeast~~ US, where isoprene is abundant. ~~(Lee et al., 2016)~~ Xu et al. (2021)  
357 observed a number of C<sub>5</sub> 1N-HOM such as C<sub>5</sub>H<sub>7,9,11</sub>NO<sub>6,7</sub> in polluted megacities of Nanjing and Shanghai of  
358 east China during summer. While many of these HOM have daytime sources and are attributed to photo-  
359 oxidation in the presence of NO<sub>x</sub>, nighttime oxidation with NO<sub>3</sub> also contribute to their formation (Lee et al.,  
360 2016; Chen et al., 2020; Xu et al., 2021).  $\text{C}_5\text{H}_{7-11}\text{NO}_{4-9}$  These compounds were also observed in chamber  
361 experiments of the reaction of isoprene with OH in the presence of  $\text{NO}_x$  (Lee et al., 2016).  $\text{C}_5\text{H}_x\text{NO}_{4-9}$  and  
362  $\text{C}_5\text{H}_x\text{NO}_{4-10}$  have been also observed in the gas phase and particle phase, respectively, in a monoterpene-  
363 dominating rural area in southwest Germany (Huang et al., 2019).

### 364 3.2.3 2N-monomers

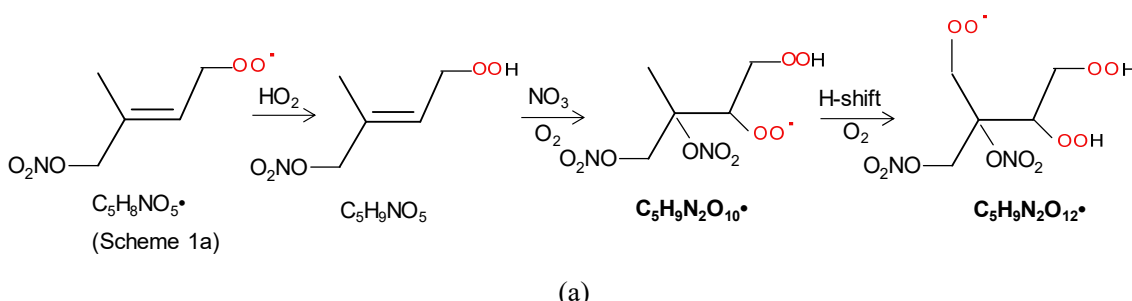
365 The 2N-monomer  $\text{RO}_2$  series  $\text{C}_5\text{H}_9\text{N}_2\text{O}_{n\bullet}$  ( $n=8-14$ ), were observed, as well as its likely termination  
366 products,  $\text{C}_5\text{H}_8\text{N}_2\text{O}_n$  and  $\text{C}_5\text{H}_{10}\text{N}_2\text{O}_n$ , which contain a carbonyl and hydroxyl or hydroperoxide functional group,  
367 respectively. The  $\text{RO}_2$  series  $\text{C}_5\text{H}_9\text{N}_2\text{O}_{n\bullet}$  with odd number of oxygen atoms ( $n=9, 11$ ) (M2a in Table 1) were  
368 likely formed from the first-generation product  $\text{C}_5\text{H}_9\text{NO}_4$  (C5-hydroxynitrate) by adding  $\text{NO}_3$  to the remaining  
369 double bond, forming  $\text{C}_5\text{H}_9\text{N}_2\text{O}_{9\bullet}$ , followed by autoxidation (Scheme 2a). This  $\text{RO}_2$  series can also be formed  
370 by the addition of  $\text{NO}_3$  to the double bond of first-generation products (e.g.  $\text{C}_5\text{H}_9\text{NO}_5$ , C5-  
371 nitrooxyhydroperoxide) and a subsequent alkoxy-peroxy step (Scheme 2b).  $\text{C}_5\text{H}_9\text{N}_2\text{O}_{n\bullet}$  with even number of  
372 oxygen atoms ( $n=8, 10, 12$ ) (M2b in Table 1), can be formed by the addition of  $\text{NO}_3$  to the double bond of  
373  $\text{C}_5\text{H}_9\text{NO}_5$  followed by autoxidation (Scheme. 3a), or of  $\text{C}_5\text{H}_9\text{NO}_4$  followed by an alkoxy-peroxy step (Scheme.  
374 3b). The formation pathways of  $\text{C}_5\text{H}_9\text{N}_2\text{O}_{13/14\bullet}$  and  $\text{C}_5\text{H}_9\text{N}_2\text{O}_{8\bullet}$  cannot be well explained, as they contain too  
375 many or too few oxygen atoms to be formed via the pathways in Scheme 2 or 3. In Scheme 2 and 3, we show the  
376 reactions starting from 1- $\text{NO}_3$ -isoprene-4-OO as an example. In the supplement, we have also shown the pathways  
377 starting from 1- $\text{NO}_3$ -isoprene-2-OO peroxy radicals, which is indicated in a recent study by Vereecken et al. (2021)  
378 to be the dominant  $\text{RO}_2$  in the reaction of isoprene with  $\text{NO}_3$ .

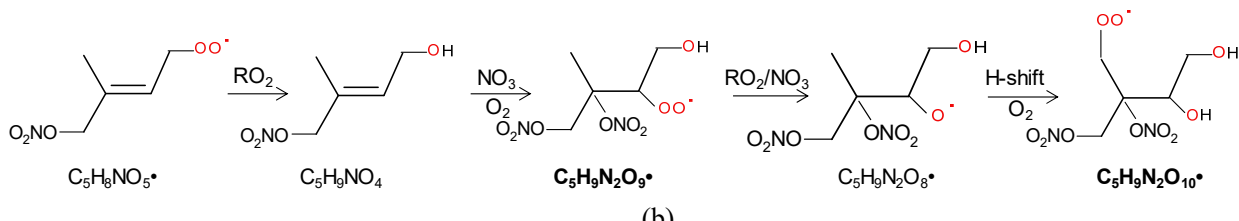
379 Formation through either Scheme 2 or 3 means that  $\text{C}_5\text{H}_8\text{N}_2\text{O}_n$  and  $\text{C}_5\text{H}_{10}\text{N}_2\text{O}_n$  were second-generation  
380 products. The time series of  $\text{C}_5\text{H}_{10}\text{N}_2\text{O}_n$  species clearly indicates that they were indeed second-generation  
381 products.  $\text{C}_5\text{H}_{10}\text{N}_2\text{O}_n$  species generally did not increase immediately with isoprene addition (Fig. 3b), but

382 increased gradually with time and reached its maximum in the later stage of each period before decreasing with  
 383 time (in the period 1 and 6), or decreasing after the next isoprene addition (periods 2-5). This time profile can  
 384 be explained by the time series of the precursor of  $C_5H_{10}N_2O_n$ ,  $C_5H_9N_2O_n\cdot$  ( $RO_2$ ) (Fig. S6). The changing rate  
 385 (production rate minus destruction rate) of  $C_5H_{10}N_2O_n$  concentration was dictated by the concentration of  
 386  $C_5H_9N_2O_n\cdot$  and the wall loss rate. During periods 2 to 5,  $C_5H_9N_2O_n\cdot$  gradually increased but decreased sharply  
 387 after the isoprene additions, resulted from chemical reactions of  $C_5H_9N_2O_n\cdot$  and additionally from wall loss.  
 388 When the rate of change of the  $C_5H_{10}N_2O_n$  concentration was positive, the concentration of  $C_5H_{10}N_2O_n$  increased  
 389 with time. After isoprene additions, the rate of change of the  $C_5H_{10}N_2O_n$  concentration decreased dramatically  
 390 to even negative, leading to decreasing concentrations. Similar to  $C_5H_{10}N_2O_n$ , the  $C_5H_8N_2O_n$  series did not  
 391 respond immediately to isoprene additions (Fig. S7), which is expected for second-generation products  
 392 according to the mechanism discussed above (Scheme 2-3). Particularly, the continuing increase of  $C_5H_8N_2O_n$   
 393 even after isoprene was completely depleted (at ~21:40, Fig. S7) clearly indicates that these compounds were  
 394 second-generation products, although in the end they decreased due to wall loss.



Scheme 2. The example pathways to form  $C_5H_9N_2O_n$  ( $n=9, 11$ ) HOM  $RO_2$  series by  $RO_2$  channel (a) and alkoxy-peroxy channel. The detected products are in bold.





408 According to the finding of Ng et al. (2008), C5-hydroxynitrate decays much faster than C5-  
409 nitrooxyhydroperoxides. Additionally, C5-hydroxynitrate concentration is expected to be higher than that of  
410 nitrooxyhydroperoxides because  $RO_2+RO_2$  forming alcohol is likely more important than  $RO_2+HO_2$  forming  
411 hydroperoxide in this study. Therefore, it is likely that  $C_5H_9N_2O_n\bullet$  M2a series was mainly formed from  $C_5H_9NO_4$   
412 instead of  $C_5H_8NO_5$ , while  $C_5H_9N_2O_n\bullet$  M2b were formed from  $C_5H_9NO_4$  followed by an alkoxy-peroxy step.  
413 That is, Scheme 2a and 3b appear more likely.

414 Similar to  $C_5H_8NO_n\bullet$ , the intensity of carbonyl species from  $C_5H_9N_2O_n\bullet$  was also comparable with that  
415 of hydroxyl/hydroperoxide species, suggesting that  $RO_2+RO_2$  reaction forming ketone and alcohol was likely  
416 an important pathway of HOM formation in the isoprene+ $NO_3$  reaction. In general, the intensity of the  
417 termination products from  $C_5H_9N_2O_n\bullet$  with both even and odd oxygen numbers were comparable. This again  
418 suggests that both peroxy and alkoxy-peroxy pathways were important for HOM formation in the isoprene+ $NO_3$   
419 reaction. The intensity of  $C_5H_8N_2O_n$  first increased and then decreased with oxygen number while  $C_5H_{10}N_2O_n$   
420 decreased with oxygen number, with  $C_5H_{10}N_2O_8$  and  $C_5H_8N_2O_8$  being the most abundant within their respective  
421 series.

422 Some 2N-monomers have been detected in previous studies of the reaction of isoprene with  $NO_3$ .  
423  $C_5H_{10}N_2O_8$  has been detected in the particle phase by Ng et al. (2008) and  $C_5H_8N_2O_7$  was detected in the gas  
424 phase by Kwan et al. (2012).  $C_5H_9N_2O_9\bullet$  has been proposed to be formed via the pathway as in Scheme 2a (Ng  
425 et al., 2008), and it was directly detected in our study.  $C_5H_8N_2O_7$  species has been proposed to be a dinitrooxy  
426 epoxide formed by the oxidation of nitrooxyhydroperoxide (Kwan et al., 2012), instead of being a dinitrooxy  
427 ketone proposed in our study, a termination product of  $C_5H_9N_2O_8\bullet$ . Admittedly,  $C_5H_8N_2O_7$  may contain both  
428 isomers. In addition, Ng et al. (2008) detected  $C_5H_8N_2O_6$  in the gas phase, which was not detected in this study  
429 likely due to the selectivity of  $NO_3^-$ -CIMS. 2N-monomers have also been observed in previous field studies.  
430 For example, Massoli et al. (2018) observed  $C_5H_{10}N_2O_{8-10}$  in rural Alabama US during the SOAS campaign. Xu  
431 et al. (2021) observed  $C_5H_{8,10}N_2O_8$  and  $C_5H_{10}N_2O_8$  in polluted megacities of Nanjing and Shanghai during  
432 summer.

433 One could suppose that  $C_5H_7N_2O_n\bullet$  should also be formed since C5-nitrooxycarbonyl ( $C_5H_7NO_4$ ) also  
434 contains one double bond that can be attacked by  $NO_3$  in a second oxidation step. However, concentrations of  
435  $C_5H_7N_2O_n$  were too low to assign molecular formulas with confidence except for  $C_5H_7N_2O_9\bullet$ , clearly showing  
436 that  $C_5H_7N_2O_n\bullet$  was not important. This fact is consistent with the finding of Ng et al. (2008) that C5-

437 nitrooxycarbonyls react slowly with  $\text{NO}_3$ . Additionally, the peroxy radical formed in the reaction of C5-  
438 nitrooxycarbonyls with  $\text{NO}_3$  likely leads to more fragmentation in H-shift as found in the OH oxidation of  
439 methacrolein (Crounse et al., 2012), which may also contribute to the low abundance of  $\text{C}_5\text{H}_7\text{N}_2\text{O}_n$ . The presence of  
440 HOM containing two N atoms is in line with the finding by Faxon et al. (2018) who detected products containing  
441 two N atoms in the reaction of  $\text{NO}_3$  with limonene, which also contain two carbon double bonds. It is anticipated  
442 that for VOC with more than one double bond,  $\text{NO}_3$  can add to all the double bonds as for isoprene and limonene.

443 **3.2.4 3N-monomers**

444 HOM containing three nitrogen atoms,  $\text{C}_5\text{H}_9\text{N}_3\text{O}_n$  ( $n=9-16$ ), were observed. These compounds were  
445 possibly peroxy nitrates formed by the reaction of  $\text{RO}_2$  ( $\text{C}_5\text{H}_9\text{N}_2\text{O}_n\bullet$ ) with  $\text{NO}_2$ . The time series of  $\text{C}_5\text{H}_9\text{N}_3\text{O}_n$   
446 was examined to check whether they match such a mechanism. If  $\text{C}_5\text{H}_9\text{N}_3\text{O}_n$  were formed by the reaction of  
447  $\text{C}_5\text{H}_9\text{N}_2\text{O}_{n-2}\bullet$  with  $\text{NO}_2$ , the concentration would be a function of the concentrations of  $\text{C}_5\text{H}_9\text{N}_2\text{O}_{n-2}\bullet$  and  $\text{NO}_2$  as  
448 follows:

$$449 \frac{d[\text{C}_5\text{H}_9\text{N}_3\text{O}_n]}{dt} = k[\text{C}_5\text{H}_9\text{N}_2\text{O}_{n-2}\bullet][\text{NO}_2] - k_{\text{wall}}[\text{C}_5\text{H}_9\text{N}_3\text{O}_n]$$

450 where  $[\text{C}_5\text{H}_9\text{N}_3\text{O}_n]$ ,  $[\text{C}_5\text{H}_9\text{N}_2\text{O}_{n-2}\bullet]$ , and  $[\text{NO}_2]$  are the concentration of these species,  $k$  is the rate  
451 constant and  $k_{\text{wall}}$  is the wall loss rate. Because the products of  $\text{C}_5\text{H}_9\text{N}_2\text{O}_{n-2}\bullet$  and  $\text{NO}_2$  were at their maximum at  
452 the end of each period and decreased rapidly after isoprene addition (Fig. S8), the concentration should have its  
453 maximum increasing rate at the end of each isoprene addition period. However, we found that only  $\text{C}_5\text{H}_9\text{N}_3\text{O}_{12}$ ,  
454 15, 16 showed such a time profile (Fig. S9), while  $\text{C}_5\text{H}_9\text{N}_3\text{O}_{9, 10, 11, 13, 14}$  generally increased with time, different  
455 from what one would expect based on the proposed pathway. Therefore, it is likely that  $\text{C}_5\text{H}_9\text{N}_3\text{O}_{12, 15, 16}$  were  
456 mainly formed via the reaction of  $\text{C}_5\text{H}_9\text{N}_2\text{O}_n\bullet$  with  $\text{NO}_2$ , whereas  $\text{C}_5\text{H}_9\text{N}_3\text{O}_{9, 10, 11, 13, 14}$  were not. Moreover,  
457  $\text{C}_5\text{H}_9\text{N}_3\text{O}_9$  cannot be explained by the reaction  $\text{C}_5\text{H}_9\text{N}_2\text{O}_n\bullet$  ( $n \geq 9$ ) with  $\text{NO}_2$  or  $\text{NO}_3$ , because these reactions  
458 would add at least one more oxygen atom. One possible pathway to form  $\text{C}_5\text{H}_9\text{N}_3\text{O}_9$  was the direct addition of  
459  $\text{N}_2\text{O}_5$  to the carbon double bond of C5-hydroxynitrate, forming a nitronitrate. Such a mechanism has been  
460 proposed previously in the heterogeneous reaction of  $\text{N}_2\text{O}_5$  with 1-palmitoyl-2-oleoyl-sn-glycero-3-  
461 phosphocholine (POPC) because  $-\text{NO}_2$  and  $-\text{NO}_3$  groups were detected (Lai and Finlayson-Pitts, 1991). This  
462 pathway generally matched the time series of  $\text{C}_5\text{H}_9\text{N}_3\text{O}_{9, 10, 11, 13, 14}$  typical of second-generation products since  
463 C5-hydroxynitrate was a first-generation product. It is possible that the main pathway of  $\text{C}_5\text{H}_9\text{N}_3\text{O}_{9, 10, 11, 13, 14}$  was  
464 the reaction of  $\text{C}_5\text{H}_9\text{NO}_{4.5, 6}$  with  $\text{N}_2\text{O}_5$ , although the reaction of  $\text{N}_2\text{O}_5$  with C=C double bonds in common alkenes  
465 and unsaturated alcohols are believed to be not important (Japar and Niki, 1975; Pfrang et al., 2006).

466 3N-monomers,  $\text{C}_5\text{H}_9\text{N}_3\text{O}_{10}$ , has been observed in the particles formed in the isoprene+ $\text{NO}_3$  reaction by  
467 Ng et al. (2008). Here a complete series of  $\text{C}_5\text{H}_9\text{N}_3\text{O}_n$  were observed.  $\text{C}_5\text{H}_9\text{N}_3\text{O}_{10}$  was previously proposed to  
468 be formed by another pathway, i.e. the reaction of  $\text{RO}_2$  ( $\text{C}_5\text{H}_9\text{N}_2\text{O}_9\bullet$ ) and  $\text{NO}_3$  (Ng et al., 2008). We further  
469 examined the possibility of such a pathway in our study. Similar to  $\text{NO}_2$ , if  $\text{C}_5\text{H}_9\text{N}_3\text{O}_n$  were formed by the  
470 reaction of  $\text{C}_5\text{H}_9\text{N}_2\text{O}_{n-2}\bullet$  with  $\text{NO}_3$ , the concentration would have its maximum increasing rate at the end of each  
471 isoprene addition period. Among  $\text{C}_5\text{H}_9\text{N}_2\text{O}_n\bullet$ , the precursors of  $\text{C}_5\text{H}_9\text{N}_3\text{O}_n$ ,  $\text{C}_5\text{H}_9\text{N}_2\text{O}_{9, 10, 13, 14}\bullet$  showed a

472 maximum increasing rate and a subsequent decrease after isoprene addition. The difference in oxygen number  
 473 between  $C_5H_9N_3O_{12, 15, 16}$ , the termination products, and  $C_5H_9N_2O_9, 10, 13, 14\bullet$ , the corresponding  $RO_2$  with the  
 474 consistent time profile is mostly two. Since the reaction of  $C_5H_9N_2O_n$  with  $NO_2$  and  $NO_3$  result an increased  
 475 oxygen number by two and by one, respectively, we infer that it is more likely that  $C_5H_9N_3O_{12, 15, 16}$  were formed  
 476 by the reaction of  $C_5H_9N_2O_{10, 13, 14}\bullet$  with  $NO_2$  rather than  $NO_3$ , and thus they were likely peroxy nitrates rather  
 477 than nitrates formed by the reaction of  $RO_2$  with  $NO_3$ . Since alkyl peroxy nitrates decompose rapidly (Finlayson-  
 478 Pitts and Pitts, 2000; Ziemann and Atkinson, 2012), it is possible that these compounds contained  
 479 peroxy acyl nitrates.

480 Little attention has been paid to the  $RO_2+NO_2$  pathway in nighttime chemistry of isoprene in the  
 481 literature (Wennberg et al., 2018), which is likely due to the instability of the products. According to this  
 482 pathway,  $C_5H_8N_2O_n$ , which was proposed to be a ketone formed via  $C_5H_9N_2O_9\bullet$  in the M2 series (Table 1) as  
 483 discussed above, can also comprise peroxy nitrates formed by the reaction of  $C_5H_8NO_n\bullet$  (M1a  $RO_2$ ) with  $NO_2$ .  
 484 3N dimer such as  $C_5H_9N_3O_{10}$  ~~or as well as 2N monomers such as  $C_5H_8N_2O_8$  and  $C_5H_8N_2O_{10}$~~  have been observed  
 485 in a recent field study in polluted cities in east China (Xu et al., 2021).<sup>a</sup>

486 **3.3 HOM dimers and their formation**

487 Table 2. HOM dimers and trimers formed in the oxidation of isoprene by  $NO_3$ .

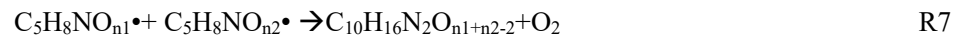
Series Number	Formula	Type	Pathway of $RO_2$
Dimer 1	$C_{10}H_{16}N_2O_{n (n=10-17)}$	ROOR <sup>a</sup>	M1 <sup>b</sup> +M1
Dimer 2	$C_{10}H_{17}N_3O_{n (n=11-19)}$	ROOR	M1+M2/M3+M4
Dimer 3	$C_{10}H_{18}N_4O_{n (n=15-18)}$	ROOR	M2+M2
Dimer 4	$C_{10}H_{18}N_2O_{n (n=10-16)}$	ROOR	M1+M4
Dimer 5	$C_{10}H_{15}N_3O_{n (n=13-17)}$	ROOR	M1+M3
Dimer 6	$C_{10}H_{19}N_3O_{n (n=14-15)}$	ROOR	M2+M4
Dimer 7	$C_{10}H_{14}N_2O_{n (n=10-16)}$	ROOR	Unknown
Dimer 8	$C_{10}H_{15}NO_{n (n=9-12)}$	ROOR	$C_{10}H_{16}NO_n$
Dimer 9	$C_{10}H_{17}NO_{n (n=9-15)}$	ROOR	$C_{10}H_{16}NO_n$
Dimer R1	$C_{10}H_{16}N_3O_{n (n=12-15)}$	$RO_2$	Dimer 1+ $NO_3$
Dimer R2	$C_{10}H_{17}N_2O_{n (n=11-12)}$	$RO_2$	Dimer 1+OH
Dimer R3	$C_{10}H_{17}N_4O_{n (n=16-18)}$	$RO_2$	Dimer 2+ $NO_3$
Dimer R4	$C_{10}H_{16}NO_{n (n=10-14)}$	$RO_2$	M1+ $C_5H_8$
Trimer 1	$C_{15}H_{24}N_4O_{n (n=17-22)}$	ROOR	Dimer R1+M1
Trimer 2	$C_{15}H_{25}N_5O_{n (n=20-22)}$	ROOR	Dimer R3+M1; Dimer R1+M2
Trimer 3	$C_{15}H_{25}N_3O_{n (n=13-20)}$	ROOR	Dimer R2+M1; Dimer R4+M2
Trimer 4	$C_{15}H_{26}N_4O_{n (n=17-21)}$	ROOR	Dimer R2+M2

488 <sup>a</sup>: ROOR denotes for organic peroxide.

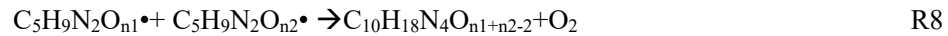
489 <sup>b</sup>: The numbering is referred to Table 1.

490 A number of HOM dimer series were observed, including  $C_{10}H_{16}N_2O_n$  ( $n=10-17$ ),  $C_{10}H_{17}N_3O_n$  ( $n=11-19$ ), and  
 491  $C_{10}H_{18}N_4O_n$  ( $n=15-18$ ),  $C_{10}H_{18}N_2O_n$  ( $n=10-16$ ),  $C_{10}H_{15}N_3O_n$  ( $n=13-17$ ), and  $C_{10}H_{19}N_3O_n$  ( $n=14-15$ ) series (Table 2,

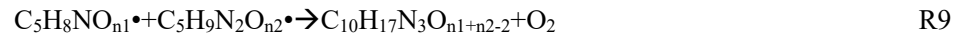
492 Table S3).  $C_{10}H_{16}N_2O_n$  series (dimer 1, Table 2) was likely formed by the accretion reaction of two monomer  $RO_2$   
 493 of M1a/b (Reaction R7).



495 Similarly,  $C_{10}H_{18}N_4O_n$  series (dimer 2, Table 2) were likely formed by the accretion reaction of two monomer  $RO_2$   
 496 of M2 (Reaction R8). As  $n_1$  and  $n_2$  are  $\geq 9$ , the number of oxygen in  $C_{10}H_{18}N_4O_n$  is expected to be  $\geq 16$ . This is  
 497 consistent with our observation that only  $C_{10}H_{18}N_4O_n$  with  $n \geq 16$  had significant concentrations.

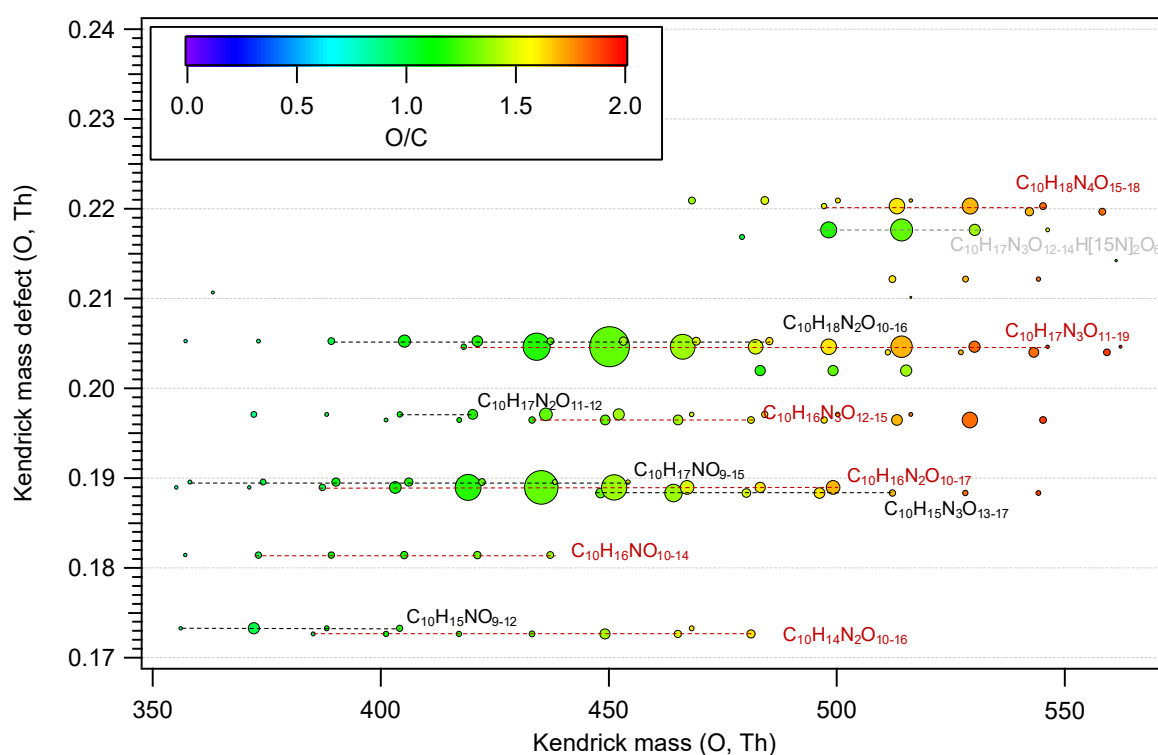


499  $C_{10}H_{17}N_3O_n$  series (dimer 3, Table 2) were likely formed by the cross accretion reaction of one M1  $RO_2$  and one  
 500 M2  $RO_2$  (reaction R9). Since  $n_1$  is  $\geq 5$  and  $n_2$  is  $\geq 9$ , the number of oxygen atoms in  $C_{10}H_{17}N_3O_n$  is expected to be  
 501  $\geq 12$ , which is also roughly consistent with our observation that only  $C_{10}H_{17}N_3O_n$  with  $n \geq 11$  were detected.



503 Similarly,  $C_{10}H_{18}N_2O_{(n=10-16)}$  and  $C_{10}H_{15}N_3O_{(n=13-17)}$  series (dimer 4, dimer 5, Table 2) were likely formed  
 504 from the accretion reaction between one M1  $RO_2$  and one M4  $RO_2$ , and between one M1  $RO_2$  and one M3  $RO_2$   
 505 ( $C_5H_7N_2O_9\bullet$ ). Other dimer series than dimer 1-5 were also present. However, they had quite low intensity (Fig. 4),  
 506 which was consistent with the low abundance of their parent monomer  $RO_2$ . They can be formed from various  
 507 accretion reactions of monomer  $RO_2$ . For example,  $C_{10}H_{19}N_3O_n$  can be formed by the accretion reaction of  
 508  $C_5H_9N_2O_{n\bullet}$  and  $C_5H_{10}NO_{n\bullet}$  (Table 2).

509 Similar to monomers, a few species dominated in HOM dimers spectrum. The dominant dimer series were  
 510  $C_{10}H_{17}N_3O_x$  and  $C_{10}H_{16}N_2O_x$  series, with  $C_{10}H_{17}N_3O_{12-14}$  and  $C_{10}H_{16}N_2O_{12-14}$  showing highest intensity among each  
 511 series (Fig. 4). In addition, the O/C ratio or oxidation state of HOM dimers were generally lower than that of  
 512 monomers (Fig. 2, Fig. 4), which resulted from the loss of two oxygen atoms in the accretion reaction of two  
 513 monomer  $RO_2$ .



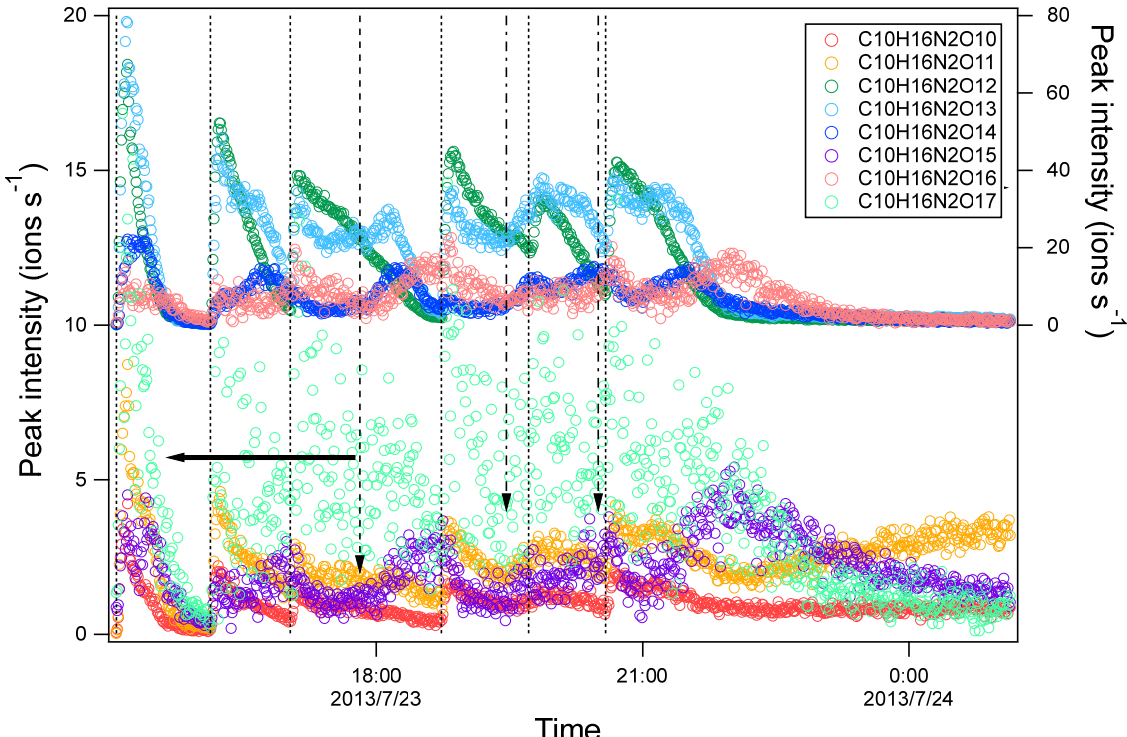
514

515       Figure 4. Kendrick mass defect plot for O of HOM dimers formed in the isoprene+NO<sub>3</sub> reaction. The size (area)  
516       of circles is set to be proportional to the average peak intensity of each molecular formula during the first isoprene addition  
517       period (P1). The molecular formula include the reagent ion <sup>15</sup>NO<sub>3</sub><sup>-</sup>, which is not shown for simplicity. The species  
518       labelled in grey (C<sub>10</sub>H<sub>17</sub>N<sub>3</sub>O<sub>12-14</sub> H[15N]<sub>2</sub>O<sub>6</sub><sup>-</sup>) are the adducts of C<sub>10</sub>H<sub>17</sub>N<sub>3</sub>O<sub>12-14</sub> with H[15N]<sub>2</sub>O<sub>6</sub><sup>-</sup>.

519       According to the mechanism above (R7-9), we attempt to explain the relative intensities of the dimers using  
520       the signal intensities of monomer RO<sub>2</sub>. Assuming that the rate constant for each of HOM-RO<sub>2</sub>+ HOM-RO<sub>2</sub> reaction  
521       forming dimers is the same considering that all HOM-RO<sub>2</sub> are highly oxygenated with a number of functional groups,  
522       it is expected that the dimer formed by the recombination between the most abundant RO<sub>2</sub> has the highest intensity.  
523       The most abundant monomer RO<sub>2</sub> were C<sub>5</sub>H<sub>9</sub>N<sub>2</sub>O<sub>9</sub><sup>•</sup> and C<sub>5</sub>H<sub>9</sub>N<sub>2</sub>O<sub>10</sub><sup>•</sup> and thus the most abundant dimers are expected  
524       to be C<sub>10</sub>H<sub>16</sub>N<sub>4</sub>O<sub>16</sub>, C<sub>10</sub>H<sub>16</sub>N<sub>4</sub>O<sub>17</sub>, and C<sub>10</sub>H<sub>16</sub>N<sub>4</sub>O<sub>18</sub>. This expected result is in contrast with our observation showing  
525       that the most abundant dimers were C<sub>10</sub>H<sub>17</sub>N<sub>3</sub>O<sub>12-14</sub> and C<sub>10</sub>H<sub>16</sub>N<sub>2</sub>O<sub>12-14</sub> (Fig. 4). The discrepancy is possibly  
526       attributed to the presence of less oxygenated RO<sub>2</sub> (with O≤5) that have a low detection sensitivity in the NO<sub>3</sub>-CIMS  
527       (Riva et al., 2019) due to their lower oxygenation compared with other HOM RO<sub>2</sub> shown above. These RO<sub>2</sub> may  
528       react with C<sub>5</sub>H<sub>9</sub>N<sub>2</sub>O<sub>9</sub><sup>•</sup> and C<sub>5</sub>H<sub>9</sub>N<sub>2</sub>O<sub>10</sub><sup>•</sup>. For example, C<sub>5</sub>H<sub>8</sub>NO<sub>5</sub><sup>•</sup> (RO<sub>2</sub>) is proposed to be an important first-  
529       generation RO<sub>2</sub> in the oxidation of isoprene by NO<sub>3</sub> (Ng et al., 2008; Rollins et al., 2009; Kwan et al., 2012;  
530       Schwantes et al., 2015). Although C<sub>5</sub>H<sub>8</sub>NO<sub>5</sub><sup>•</sup> showed very low signal in our mass spectra, it was likely to have high  
531       abundance since it was the first RO<sub>2</sub> formed in the reaction of isoprene with NO<sub>3</sub>. Indeed, we found that the  
532       termination products of C<sub>5</sub>H<sub>8</sub>NO<sub>5</sub><sup>•</sup> such as C<sub>5</sub>H<sub>9</sub>NO<sub>5</sub>, C<sub>5</sub>H<sub>7</sub>NO<sub>4</sub>, and C<sub>5</sub>H<sub>9</sub>NO<sub>4</sub> had high abundance in another study,  
533       indicating the high abundance of C<sub>5</sub>H<sub>8</sub>NO<sub>5</sub><sup>•</sup>. The accretion reaction of C<sub>5</sub>H<sub>8</sub>NO<sub>5</sub><sup>•</sup> with C<sub>5</sub>H<sub>9</sub>N<sub>2</sub>O<sub>9-10</sub><sup>•</sup> and C<sub>5</sub>H<sub>8</sub>NO<sub>9-10</sub><sup>•</sup>  
534       can explain the high abundance of C<sub>10</sub>H<sub>17</sub>N<sub>3</sub>O<sub>12-14</sub> and C<sub>10</sub>H<sub>16</sub>N<sub>2</sub>O<sub>12-14</sub> among all dimers.

535       Provided that C<sub>5</sub>H<sub>8</sub>NO<sub>5</sub><sup>•</sup> is abundant, we still cannot explain the relative intensity of C<sub>10</sub>H<sub>17</sub>N<sub>3</sub>O<sub>12</sub>,  
536       C<sub>10</sub>H<sub>17</sub>N<sub>3</sub>O<sub>13</sub>, and C<sub>10</sub>H<sub>17</sub>N<sub>3</sub>O<sub>14</sub> that were all formed by the accretion reaction with C<sub>5</sub>H<sub>8</sub>NO<sub>5</sub><sup>•</sup>. C<sub>10</sub>H<sub>17</sub>N<sub>3</sub>O<sub>12</sub> should  
537       have the highest intensity among C<sub>10</sub>H<sub>17</sub>N<sub>3</sub>O<sub>12-14</sub> as its precursor RO<sub>2</sub>, C<sub>5</sub>H<sub>9</sub>N<sub>2</sub>O<sub>9</sub><sup>•</sup>, is the most abundant. This  
538       suggests that accretion reactions other than those of C<sub>5</sub>H<sub>8</sub>NO<sub>5</sub><sup>•</sup> with C<sub>5</sub>H<sub>9</sub>N<sub>2</sub>O<sub>9-10</sub><sup>•</sup> also contributed to C<sub>10</sub>H<sub>17</sub>N<sub>3</sub>O<sub>12-14</sub>. Admittedly, the assumption of different RO<sub>2</sub> having similar rate constants in accretion reactions may not be valid.  
539       For example, self-reaction of tertiary RO<sub>2</sub> is slower than secondary and primary RO<sub>2</sub> (Jenkin et al., 1998; Finlayson-  
540       Pitts and Pitts, 2000). Different rate constants may also lead to the observation that the most abundant dimers could  
541       not be explained the most abundant RO<sub>2</sub>.

543



544

545 Figure 5. Time series of peak intensity of several HOM dimers of  $C_{10}H_{16}N_2O_n$  series. The dashed lines  
 546 indicate the time of isoprene additions. The long-dashed arrow indicates the time of  $NO_2$  addition. The dash-dotted  
 547 arrows indicate the time of  $O_3$  additions. The horizontal arrows indicate y-axis scales for different markers.

548 The time profiles of  $C_{10}H_{16}N_2O_n$  indicate contributions of both the first- and second-generation products.  
 549 The dominance of the first- or second-generation products depended on the specific compounds. Most  $C_{10}H_{16}N_2O_n$   
 550 compounds increased instantaneously after isoprene additions, indicating significant contributions of first-generation  
 551 products. Since the formation of  $C_{10}H_{16}N_2O_n$  likely involved  $C_5H_8NO_5\bullet$  as discussed above, the instantaneous  
 552 increase may result from the increase of  $C_5H_8NO_5\bullet$  as well as other first-generation  $RO_2$ . After the initial increase,  
 553  $C_{10}H_{16}N_2O_{10-12}$  then decayed with time (Fig. 5) while  $C_{10}H_{16}N_2O_{13-15}$  increased again in the later phase of a period  
 554 and when  $NO_2$  and  $O_3$  were added. The second increase indicated that  $C_{10}H_{16}N_2O_{13-15}$  may contain more than one  
 555 isomer, which had different production pathways. As discussed above,  $C_5H_8NO_5\bullet$  can be either a first-generation  
 556  $RO_2$  formed directly via the reaction of isoprene with  $NO_3$  and autoxidation, or a second-generation  $RO_2$ , e.g. formed  
 557 via the reaction of with  $C_5H_8O_2$  with  $NO_3$ . Therefore the second increase of  $C_{10}H_{16}N_2O_{13-15}$  may result from the  
 558 reaction of two first-generation  $RO_2$  and of two second-generation  $RO_2$  or between one first-generation and one  
 559 second-generation  $RO_2$ . The increase of  $C_{10}H_{16}N_2O_{14-15}$  after isoprene addition was not large, indicating the  
 560 larger contributions from second-generation products compared with other  $C_{10}H_{16}N_2O_n$ . Overall, as the number  
 561 of oxygen increased, the contribution of second-generation products to  $C_{10}H_{16}N_2O_n$  increased.

562 In contrast to  $C_{10}H_{16}N_2O_n$  series,  $C_{10}H_{18}N_4O_n$  increased gradually after each isoprene addition and then  
 563 decreased afterward (Fig. 6), either naturally or after isoprene additions, which is typical for second-generation  
 564 products. Since  $C_{10}H_{18}N_4O_n$  was likely formed by the accretion reaction of  $C_5H_9N_2O_n\bullet$  ( $RO_2$ ), the time profile  
 565 of  $C_{10}H_{18}N_4O_n$  was as expected since  $C_5H_9N_2O_n\bullet$  was formed via the reaction of  $NO_3$  with first-generation

566 products  $C_5H_9NO_n$ . The  $C_{10}H_{18}N_4O_n$  concentration depended on the product of the concentrations of two  
 567  $C_5H_9N_2O_n\bullet$ . Taking  $C_{10}H_{18}N_4O_{16}$  as an example, its concentration can be expressed as follows:

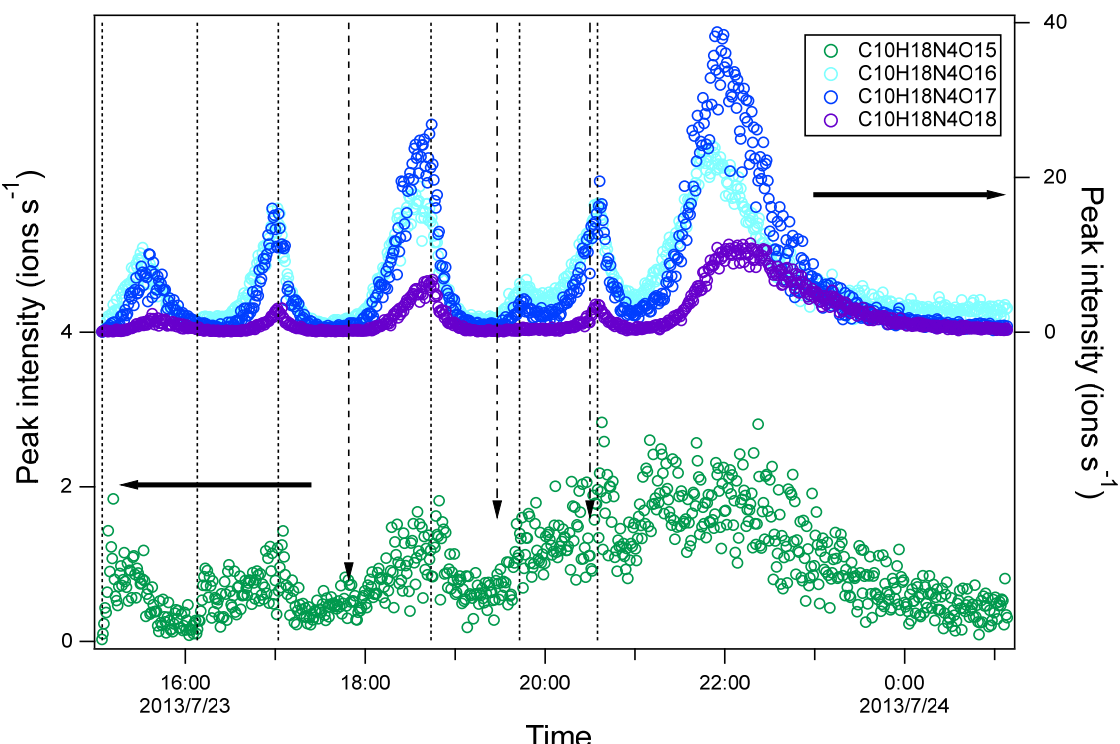
568

$$\frac{d[C_{10}H_{18}N_4O_{16}]}{dt} = k[C_5H_9N_2O_9][C_5H_9N_2O_9] - k_{wl}[C_{10}H_{18}N_4O_{16}]$$

569 When the concentration of  $C_5H_9N_2O_9\bullet$  increased, the changing rate of  $C_{10}H_{18}N_4O_{16}$  was positive and increased  
 570 and thus the concentration of  $C_{10}H_{18}N_4O_{16}$  increased. When the concentration  $C_5H_9N_2O_9\bullet$  decreased sharply  
 571 after isoprene additions, the changing rate of  $C_{10}H_{18}N_4O_{16}$  decreased and even became negative values, and thus  
 572 the concentration of  $C_{10}H_{18}N_4O_{16}$  decreased after isoprene addition.

573 Similar to the  $C_{10}H_{16}N_2O_n$  series, while  $C_{10}H_{17}N_3O_n$  first increased instantaneously with isoprene  
 574 addition, it increased again during the later stage of each period (Fig. S10), showing a mixed behavior of the  
 575 first-generation products and second-generation products. The time series of  $C_{10}H_{17}N_3O_n$  was as expected in  
 576 general because  $C_{10}H_{17}N_3O_n$  was likely formed via the accretion reaction of  $C_5H_8NO_n\bullet$  (M1 RO<sub>2</sub>) and  
 577  $C_5H_9N_2O_n\bullet$  (M2 RO<sub>2</sub>), which were first- or second-generation, and second-generation RO<sub>2</sub>, respectively,

578

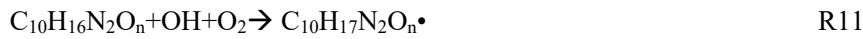
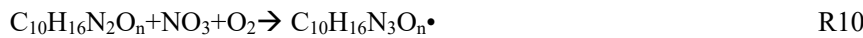


579

580 Figure 6. Time series of peak intensity of several HOM dimers of  $C_{10}H_{18}N_4O_n$  series. The dashed lines indicate the  
 581 time of isoprene additions. The long-dashed arrow indicates the time of  $NO_2$  addition. The dash-dotted arrows  
 582 indicate the time of  $O_3$  additions. The horizontal arrows indicate y-axis scales for different markers.

583 Some dimers that cannot be explained by accretion reactions such as  $C_{10}H_{16}N_3O_{n=12-15}\bullet$ ,  $C_{10}H_{17}N_2O_{n=11-12}\bullet$ ,  
 584  $C_{10}H_{16}NO_{n=10-14}\bullet$ ,  $C_{10}H_{15}NO_{n=9-12}$ ,  $C_{10}H_{17}NO_{n=9-15}$  were also observed. These dimers had low abundance.  
 585 We note that due to their low signals in the mass spectra, their assignment and thus range of n may be subject to  
 586 uncertainties. Since  $C_{10}H_{16}NO_{n=10-16}\bullet$ ,  $C_{10}H_{16}N_3O_{n=12-15}\bullet$ , and  $C_{10}H_{17}N_2O_n\bullet$  contain unpaired electrons, they

587 cannot be formed via the direct accretion reaction of two  $\text{RO}_2$ . Instead,  $\text{C}_{10}\text{H}_{16}\text{N}_3\text{O}_{\text{n}}$  (n=12-15)  $\bullet$  (dimer R1) and  
588  $\text{C}_{10}\text{H}_{17}\text{N}_2\text{O}_{\text{n}}\bullet$  (dimer R2) were likely  $\text{RO}_2$  formed by the reaction of HOM dimers containing a double bond (dimer  
589 1) with  $\text{NO}_3$  and with OH, respectively, followed by the reaction with  $\text{O}_2$ .



592 The corresponding termination products of  $\text{C}_{10}\text{H}_{16}\text{N}_3\text{O}_{\text{n}}\bullet$   $\text{RO}_2$  series such as  $\text{C}_{10}\text{H}_{15}\text{N}_3\text{O}_{\text{n}}$  (ketone),  $\text{C}_{10}\text{H}_{17}\text{N}_3\text{O}_{\text{n}}$   
593 (hydroperoxide/alcohol) were also observed, although these compounds can also be formed via reactions between  
594 two  $\text{RO}_2$  radicals (R9 and R11). Among the termination products,  $\text{C}_{10}\text{H}_{15}\text{N}_3\text{O}_{\text{n}}$  had low intensity. Reaction R13 and  
595 the termination reaction of  $\text{C}_{10}\text{H}_{17}\text{N}_2\text{O}_{\text{n}}\bullet$  with  $\text{HO}_2$  provided an additional pathway to  $\text{C}_{10}\text{H}_{17}\text{N}_3\text{O}_{\text{n}}$  besides the R9  
596 pathway discussed above. Similarly, other dimers may also be formed by the termination reactions of dimer  $\text{RO}_2$   
597 with  $\text{RO}_2$  or  $\text{HO}_2$ . E.g.,  $\text{C}_{10}\text{H}_{18}\text{N}_4\text{O}_{\text{n}}$  can be formed via termination reaction of  $\text{C}_{10}\text{H}_{17}\text{N}_4\text{O}_{\text{n}}\bullet$  with another  $\text{RO}_2$  wherein  
598  $\text{C}_{10}\text{H}_{17}\text{N}_4\text{O}_{\text{n}}\bullet$  can be formed as follows:



600  $\text{C}_{10}\text{H}_{16}\text{NO}_{\text{n}}$  (n=10-14)  $\bullet$  could be explained by the reaction of monomer  $\text{RO}_2$  with isoprene.



602 Only  $\text{C}_{10}\text{H}_{16}\text{NO}_{\text{n}}\bullet$  with  $n \geq 10$  were detected, while according to the mechanism of self-reaction between  $\text{C}_5\text{H}_8\text{NO}_{\text{n}}\bullet$ ,  
603 the n range of  $\text{C}_{10}\text{H}_{16}\text{NO}_{\text{n}}\bullet$  is expected to be 7-14. The absence of  $\text{C}_{10}\text{H}_{16}\text{NO}_{\text{n}}\bullet$  (n<10) is likely attributed to their low  
604 abundance, which might result from low precursor concentrations, low reaction rates with isoprene, and/or faster  
605 reactive losses with other radicals. Such a reaction of  $\text{RO}_2$  with isoprene has been proposed by Ng et al. (2008) and  
606 Kwan et al. (2012). The corresponding termination products of  $\text{C}_{10}\text{H}_{16}\text{NO}_{\text{n}}\bullet$  are  $\text{C}_{10}\text{H}_{15}\text{NO}_{\text{n}}$  (ketone) and  $\text{C}_{10}\text{H}_{17}\text{NO}_{\text{n}}$   
607 species (hydroperoxide/alcohol).  $\text{C}_{10}\text{H}_{17}\text{NO}_{\text{n}}$  species showed a time profile of typical first-generation products (Fig.  
608 S11), i.e. increasing immediately with isoprene addition and then decaying with time. This behaviour further supports  
609 the possibility of reaction R13. Yet, the reaction rate of alkene with  $\text{RO}_2$  is likely low due to the high activation  
610 energy (Stark, 1997, 2000). It is worth noting that to our knowledge no experimental kinetic data on the addition of  
611  $\text{RO}_2$  to alkenes in the gas phase in atmospheric relevant conditions are available, though fast, low-barrier ring closure  
612 reactions in unsaturated  $\text{RO}_2$  radicals have been reported (Vereecken and Peeters, 2004, 2012; Kaminski et al., 2017;  
613 Richters et al., 2017; Chen et al., 2021). We would like to note that there is unlikely interference to  $\text{C}_{10}\text{-HOM}$  from  
614 monoterpenes, which has been reported previously (Bernhammer et al., 2018), as the concentration of monoterpenes  
615 in the chamber during this study was below the limit of detection, which was  $\sim 50$  ppt ( $3\sigma$ ).

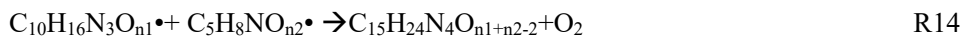
616 Some of the dimers discussed above have been observed in previous laboratory studies. Ng et al. (2008)  
617 found  $\text{C}_{10}\text{H}_{16}\text{N}_2\text{O}_8$  and  $\text{C}_{10}\text{H}_{16}\text{N}_2\text{O}_9$  in the gas phase and  $\text{C}_{10}\text{H}_{17}\text{N}_3\text{O}_{12}$ ,  $\text{C}_{10}\text{H}_{17}\text{N}_3\text{O}_{13}$ ,  $\text{C}_{10}\text{H}_{18}\text{N}_4\text{O}_{16}$ , and  $\text{C}_{10}\text{H}_{17}\text{N}_5\text{O}_{18}$   
618 in the particle phase.  $\text{C}_{10}\text{H}_{16}\text{N}_2\text{O}_8$  and  $\text{C}_{10}\text{H}_{16}\text{N}_2\text{O}_9$  were also observed in our study, but their intensity in the MS was  
619 too low to assign molecular formulas with high confidence. The low intensity may be due to the low sensitivity of  
620  $\text{C}_{10}\text{H}_{16}\text{N}_2\text{O}_{8,9}$  in  $\text{NO}_3^-$ -CIMS. According to modelling results of the products formed in cyclohexene ozonolysis by  
621 Hyttinen et al. (2015), at least two hydrogen bond donor functional groups are needed for a compound to be detected  
622 in a nitrate CIMS. As  $\text{C}_{10}\text{H}_{16}\text{N}_2\text{O}_8$  and  $\text{C}_{10}\text{H}_{16}\text{N}_2\text{O}_9$  have no and only one H-bond donor function groups, respectively,  
623 they are expected to have low sensitivity in  $\text{NO}_3^-$ -CIMS. Moreover, the low intensity can be partly attributed to the  
624 much lower isoprene concentrations used in this study compared to previous studies, leading to the low concentration

625 of  $C_{10}H_{16}N_2O_8$  and  $C_{10}H_{16}N_2O_9$  (Ng et al., 2008).  $C_{10}H_{17}N_3O_{12}$ ,  $C_{10}H_{17}N_3O_{13}$ ,  $C_{10}H_{18}N_4O_{16}$ , and  $C_{10}H_{17}N_5O_{18}$  were  
626 all observed in the gas phase in this study, wherein the concentration of  $C_{10}H_{17}N_5O_{18}$  was very low. The formation  
627 pathways of  $C_{10}H_{17}N_3O_{12}$ ,  $C_{10}H_{17}N_3O_{13}$ , and  $C_{10}H_{18}N_4O_{16}$  (R8) were generally similar to those proposed by Ng et al.  
628 (2008) except that the products from H-shift of  $RO_2$  were involved in the formation of  $C_{10}H_{17}N_3O_{13}$ . Among the two  
629 pathways of  $C_{10}H_{18}N_4O_{16}$  formation (R8 and via R12), our results indicate that R8 was the main pathway, based on  
630 the low concentrations of  $C_{10}H_{17}N_4O_{16/17}\cdot$  and other termination product of them,  $C_{10}H_{16}N_4O_{15/16}$ . That the time  
631 profile of  $C_{10}H_{18}N_4O_{16}$  was consistent with what is expected from R8 as discussed above offers additional evidence  
632 to that conclusion.

633 Few field studies have reported HOM dimers formed via the reaction  $NO_3$  with isoprene. This might be  
634 because  $NO_3$ +isoprene-HOM dimers can have the identical molecular formula to the HOM monomers from  
635 monoterpene oxidation. Possible contribution of dimer formation in the isoprene oxidation to C6-10 HOM in the  
636 particle phase observed at a rural site Yorkville, US is reported by Chen et al. (2020), although these HOM are  
637 attributed to be more likely from monoterpene oxidation.

### 638 3.4 HOM trimers and their formation

639 A series of HOM trimers were observed, such as  $C_{15}H_{24}N_4O_n$  ( $n=17-22$ ),  $C_{15}H_{25}N_5O_n$  ( $n=20-22$ ),  $C_{15}H_{25}N_3O_n$   
640 ( $n=13-20$ ),  $C_{15}H_{26}N_4O_n$  ( $n=17-21$ ), and  $C_{15}H_{24}N_2O_n$  ( $n=12-16$ ). Among the trimers,  $C_{15}H_{24}N_4O_n$  was the most abundant series  
641 (Fig. S12). The  $C_{15}H_{24}N_4O_n$  series can be explained by the accretion reaction of one monomer HOM  $RO_2$  and  
642 one dimer HOM  $RO_2$ .



643 The formation pathways of dimer  $RO_2$   $C_{10}H_{16}N_3O_n$  ( $n=12-15$ ) and  $C_{10}H_{17}N_2O_n$  are shown above (reaction R10 and  
644 R11).

645 The other trimers were likely formed via similar pathways (Table 2 and Supplement S2). Since  $NO_3^-$ -CIMS  
646 cannot provide the structural information of these HOM trimers, we cannot elucidate the major pathways. However,  
647 in all these pathways, dimer- $RO_2$  is necessary to form a trimer, and most of the dimer- $RO_2$  formation pathways  
648 require at least one double bond in the dimer molecule except for the reaction of  $RO_2$  with isoprene. Since one  
649 double bond has already reacted in the monomer- $RO_2$  formation, we anticipate that in the reaction with  $NO_3$  it is  
650 more favourable for precursors (VOC) containing more than one double bonds to form trimer molecules than  
651 precursors containing only one double bond, as it is easier to generate new  $RO_2$  radicals from these dimers by  
652 attack on the remaining double bond(s).

653 The time profile of  $C_{15}H_{24}N_4O_n$  showed the mixed behavior of first- and second-generation products (Fig.  
654 S13), consistent with the mechanism discussed above since  $C_5H_8NO_n\cdot$  and  $C_{10}H_{16}N_3O_n\cdot$  were of first- or second-  
655 generation and second-generation, respectively. The contributions of the second-generation products became  
656 larger as the number of oxygen atoms increased. In contrast,  $C_{15}H_{25}N_3O_n$  showed instantaneous increase with  
657 isoprene addition (Fig. S14), which was typical for time profiles of first-generation products. Both proposed  
658 formation pathways of  $C_{15}H_{25}N_3O_n$  (RS6 and RS7) contained a second-generation  $RO_2$ , which was not in line with  
659 the time profile observed. The observation cannot be well explained, unless we assume molecular adducts of a dimer

661 with one monomer. It is also possible that some  $C_{10}H_{17}N_2O_n\bullet$  were formed very fast or that there were other  
662 formation pathways of  $C_{15}H_{25}N_3O_n$  not accounted for here.

663 We are not aware of field studies reporting  $NO_3$ +isoprene-HOM trimers, which is likely due to the same  
664 reason for dimers discussed above. It is challenging to distinguish HOM trimers formed in the reaction  $NO_3$  with  
665 isoprene from the dimers formed by cross reaction of the  $RO_2$  from monoterpene oxidation (C10- $RO_2$ ) with that from  
666 isoprene oxidation (C5- $RO_2$ ) as their molecular formula can be identical.

### 667 3.5 Contributions of monomers, dimer, and trimers to HOM

668 The concentration (represented by peak intensity) of monomers was higher than that of dimers, but overall  
669 their concentrations remained of the same order of magnitude (Fig 1a, inset). The concentration of trimers was much  
670 lower than that of monomers and dimers. The relative contributions of monomers, dimers, and trimers evolved in  
671 time due to the changing concentration of each HOM species. Comparing the contributions of various classes of  
672 HOM in period 1 with those in periods 1-6 reveals that the relative contribution of monomers increased with time,  
673 especially that of 2N-monomers, while the contribution of dimers decreased. This trend is attributed to the larger wall  
674 loss of dimers compared to monomers because of their lower volatility and also to the continuous formation of  
675 second-generation monomers, mostly 2N-monomers. Overall, the relative contribution of total HOM monomers  
676 decreased immediately after isoprene addition while the contribution of HOM dimers increased rapidly (Fig. S15),  
677 which was attributed to the faster increase of dimers intensity due to their rapid formation. Afterwards, the  
678 contribution of monomers to total HOM gradually increased and that of dimers decreased, which was partly due to  
679 the faster wall loss rate of dimers and to the continuous formation of second-generation monomers.

### 680 3.6 Yield of HOM

681 The HOM yield in the oxidation of isoprene by  $NO_3$  was estimated using the sensitivity of  $H_2SO_4$ . It was  
682 derived for the first isoprene addition period to minimize the contribution of multi-generation products and to better  
683 compare with the data in literature, thus denoted as primary HOM yield (Pullinen et al., 2020) and was estimated to  
684 be  $1.2\%_{-0.7\%}^{+1.3\%}$ . The uncertainty was estimated as shown in the Supplement S1. Despite the uncertainty, the primary  
685 HOM yield here was much higher than the HOM yield from the ozonolysis and photooxidation of isoprene (Jokinen  
686 et al., 2015). The difference may be attributed to the more efficient oxygenation in the addition of  $NO_3$  to carbon  
687 double bonds. Compared with the reaction with  $O_3$  or  $OH$ , the initial peroxy radicals contains 5 oxygen atoms when  
688 isoprene reacts with  $NO_3$ , while the initial peroxy radicals contains only 3 oxygen atoms when reacting with  $OH$ , and  
689 the ozonide contains 3 oxygen atoms in the case of  $O_3$ .

## 690 4 Conclusion and implications

691 HOM formation in the reaction of isoprene with  $NO_3$  was investigated in the SAPHIR chamber. A number  
692 of HOM monomers, dimers, and trimers containing one to five nitrogen atoms were detected, and their time-  
693 dependent concentration profiles were tracked throughout the experiment. Some formation mechanisms for various  
694 HOM were proposed according to the molecular formula identified, and the available literature. HOM showed a  
695 variety of time profiles with multiple isoprene additions during the reaction. First-generation HOM increased

instantaneously after isoprene addition and then decreased while second-generation HOM increased gradually and then decreased with time, reaching a maximum concentration at the later stage of each period. The time profiles provide additional constraints on their formation mechanism beside the molecular formula, suggesting whether they were first-generation products or second-generation products or a combination of both. 1N-monomers (mostly C<sub>5</sub>) were likely formed by NO<sub>3</sub> addition to a double bond of isoprene, forming monomer RO<sub>2</sub>, followed by autoxidation and termination via the reaction with HO<sub>2</sub>, RO<sub>2</sub>, and NO<sub>3</sub>. Time series suggest that some 1N-monomer could also be formed by the reaction of first-generation products with NO<sub>3</sub>, and thus be of second-generation. 2N-monomers were likely formed via the reaction of first-generation products such as C5-hydroxynitrate with NO<sub>3</sub> and thus second-generation products. 3N-monomers likely comprised peroxy/peroxyacetyl nitrates formed by the reaction of 2N-monomer RO<sub>2</sub> with NO<sub>2</sub>, and possibly nitronitrates formed via the direct addition of N<sub>2</sub>O<sub>5</sub> to the first-generation products. HOM dimers were mostly formed by the accretion reactions between various HOM monomer RO<sub>2</sub>, either first-generation or second-generation or with the contributions of both, and thus showed time profiles typical of either first-generation products, or second-generation products, or a combination of both. Additionally, some dimers peroxy radicals (dimer RO<sub>2</sub>) were formed by the reaction of NO<sub>3</sub> with dimers containing a C=C double bond. HOM trimers were proposed to be formed by accretion reactions between the monomer RO<sub>2</sub> and dimer RO<sub>2</sub>.

Overall, both HOM monomers and dimers contribute significantly to total HOM while trimers only contributed a minor fraction. Within both the monomer and dimer compounds, a limited set of compounds dominated the abundance, such as C<sub>5</sub>H<sub>8</sub>N<sub>2</sub>O<sub>n</sub>, C<sub>5</sub>H<sub>10</sub>N<sub>2</sub>O<sub>n</sub>, C<sub>10</sub>H<sub>17</sub>N<sub>3</sub>O<sub>n</sub>, and C<sub>10</sub>H<sub>16</sub>N<sub>2</sub>O<sub>n</sub> series. 2N-monomers, which were second-generation products, dominated in monomers and accounted for ~34% of all HOM, indicating the important role of second-generation oxidation in HOM formation in the isoprene+NO<sub>3</sub> reaction. Both RO<sub>2</sub> autoxidation and “alkoxy-peroxy” pathways were found to be important for 1N- and 2N-HOM formation. In total, the yield of HOM monomers, dimers, and trimers accounted for 1.3%<sup>+1.3%</sup><sub>-0.7%</sub> of the isoprene reacted, which was much higher than the HOM yield in the oxidation of isoprene by OH and O<sub>3</sub> reported in the literature (Jokinen et al., 2015). This means that the reaction of isoprene with NO<sub>3</sub> is a competitive pathway of HOM formation from isoprene.

The HOM in the reaction of isoprene with NO<sub>3</sub> may account for a significant fraction of SOA. If all the HOM condense on particles, using the molecular weight of the HOM with the least molecular weight observed in this study (C<sub>5</sub>H<sub>9</sub>NO<sub>6</sub>), the HOM yield corresponds to a SOA yield of 3.6%. Although SOA concentrations were not measured in this study, Ng et al. (2008) reported a SOA yield of the isoprene+NO<sub>3</sub> reaction of 4.3%-23.8%. Rollins et al. (2009) reported a SOA yield of 2% at low organic aerosol loading (~0.52 μg m<sup>-3</sup>) and 14% if the further oxidation of the first-generation products are considered in the isoprene+NO<sub>3</sub> reaction. Comparing the potential SOA yield produced by HOM with SOA yields in the literature suggests that HOM may play an important role in the SOA formation in the isoprene+NO<sub>3</sub> reaction.

The RO<sub>2</sub> lifetime is approximately 20-50 s in our experiments, which is generally comparable or shorter than the lifetime of RO<sub>2</sub> in the ambient atmosphere at night, varying from several 10 s to several 100 s (Fry et al., 2018), depending on the NO<sub>3</sub>, HO<sub>2</sub>, and RO<sub>2</sub> concentrations. Assuming a HO<sub>2</sub>, RO<sub>2</sub>, and NO<sub>3</sub> concentration of 5 ppt, 5 ppt (Tan et al., 2019), and 300 ppt (Brown and Stutz, 2012) respectively, the RO<sub>2</sub> lifetime in our study is comparable to the nighttime RO<sub>2</sub> lifetime (50 s) found in urban locations and areas influenced by urban plume. In areas with longer RO<sub>2</sub> lifetime such as remote areas, the autoxidation is expected to be more important relative to bimolecular reactions.

734 This may enhance HOM yield and thus enhance SOA yield. However, on the other hand, at lower RO<sub>2</sub> concentration  
735 and thus longer RO<sub>2</sub> lifetime, reduced rates of RO<sub>2</sub>+RO<sub>2</sub> reactions producing low-volatility dimers can reduce the  
736 SOA yield via reducing dimer yield (McFiggans et al., 2019; Pullinen et al., 2020). The RO<sub>2</sub> fate in our experiments  
737 is dominated the reaction RO<sub>2</sub>+NO<sub>3</sub> with significant contribution of RO<sub>2</sub>+RO<sub>2</sub>, which can also represent the RO<sub>2</sub> fate  
738 in the urban areas and areas influenced by urban plume. Our experiment condition cannot represent the chemistry in  
739 HO<sub>2</sub>-dominated regions such as clean forest environment (Schwantes et al., 2015).

740 We observed the second-generation products formed by the reaction of first-generation products. The  
741 lifetime of first-generation nitrates in the ambient atmosphere, according their rate constants with OH and NO<sub>3</sub>  
742 (Wennberg et al., 2018), are ~5 h and ~1.3-4 h, respectively, with respect to the reaction with OH and NO<sub>3</sub> assuming  
743 a typical OH concentration of  $2 \times 10^6$  molecules cm<sup>-3</sup> (Lu et al., 2014; Tan et al., 2019) and NO<sub>3</sub> concentration of 100-  
744 300 ppt in urban areas (Brown and Stutz, 2012). Therefore, they have the chance to react further with OH and NO<sub>3</sub>  
745 at dawn. In our experiments, the lifetimes of these first-generation nitrates with respect to OH and NO<sub>3</sub> are  
746 comparable to the aforementioned lifetime due to comparable OH and NO<sub>3</sub> concentrations with these ambient  
747 conditions. Therefore, our findings on the second-generation products are relevant to the ambient urban atmosphere  
748 and areas influenced by urban plumes. Some of these products such as C<sub>5</sub>H<sub>8</sub><sub>10</sub>N<sub>2</sub>O<sub>8</sub> and multi-generation  
749 nitrooxyorganosulfates have been observed in recent field studies in polluted megacities in east China (Hamilton et  
750 al., 2021; Xu et al., 2021).

## 751 **Data availability**

752 All the data in the figures of this study are available upon request to the corresponding author (t.mentel@fz-juelich.  
753 de or dfzhao@fudan.edu.cn).

## 754 **Competing interests**

755 The authors declare that they have no conflict of interest.

## 756 **Author contribution**

757 TFM, HF, SS, DZ, IP, AW, and AKS designed the experiments. Instrument deployment and operation were carried  
758 out by IP, HF, SS, IA, RT, FR, DZ, and RW. Data analysis was done by DZ, HF, SS, RW, IA, RT, FR, YG, SK. DZ,  
759 TFM, RW, JW, SK, and LV interpreted the compiled data set. DZ and TFM wrote the paper. All co-authors discussed  
760 the results and commented on the paper.

## 761 **Acknowledgements**

762 We thank the SAPHIR team for supporting our measurements and providing helpful data. D. Zhao and Y. Guo would  
763 like to thank the support of National Natural Science Foundation of China (41875145). We would like to thank three  
764 anonymous reviewers and Kristian Møller for their helpful comments.

## References

- Atkinson, R., Baulch, D. L., Cox, R. A., Crowley, J. N., Hampson, R. F., Hynes, R. G., Jenkin, M. E., Rossi, M. J., and Troe, J.: Evaluated kinetic and photochemical data for atmospheric chemistry: Volume II - gas phase reactions of organic species, *Atmos. Chem. Phys.*, 6, 3625-4055, 2006.
- Ayres, B. R., Allen, H. M., Draper, D. C., Brown, S. S., Wild, R. J., Jimenez, J. L., Day, D. A., Campuzano-Jost, P., Hu, W., de Gouw, J., Koss, A., Cohen, R. C., Duffey, K. C., Romer, P., Baumann, K., Edgerton, E., Takahama, S., Thornton, J. A., Lee, B. H., Lopez-Hilfiker, F. D., Mohr, C., Wennberg, P. O., Nguyen, T. B., Teng, A., Goldstein, A. H., Olson, K., and Fry, J. L.: Organic nitrate aerosol formation via  $\text{NO}_3 +$  biogenic volatile organic compounds in the southeastern United States, *Atmos. Chem. Phys.*, 15, 13377-13392, 10.5194/acp-15-13377-2015, 2015.
- Berndt, T., and Böge, O.: Gas-phase reaction of  $\text{NO}_3$  radicals with isoprene: a kinetic and mechanistic study, *Int. J. Chem. Kinet.*, 29, 755-765, 10.1002/(sici)1097-4601(1997)29:10<755::Aid-kin4>3.0.co;2-1, 1997.
- Berndt, T., Mender, B., Scholz, W., Fischer, L., Herrmann, H., Kulmala, M., and Hansel, A.: Accretion Product Formation from Ozonolysis and OH Radical Reaction of alpha-Pinene: Mechanistic Insight and the Influence of Isoprene and Ethylene, *Environ. Sci. Technol.*, 52, 11069-11077, 10.1021/acs.est.8b02210, 2018a.
- Berndt, T., Scholz, W., Mentler, B., Fischer, L., Herrmann, H., Kulmala, M., and Hansel, A.: Accretion Product Formation from Self- and Cross-Reactions of  $\text{RO}_2$  Radicals in the Atmosphere, *Angew. Chem.-Int. Edit.*, 57, 3820-3824, 10.1002/anie.201710989, 2018b.
- Bernhammer, A. K., Fischer, L., Mentler, B., Heinritzi, M., Simon, M., and Hansel, A.: Production of highly oxygenated organic molecules (HOMs) from trace contaminants during isoprene oxidation, *Atmos. Meas. Tech.*, 11, 4763-4773, 10.5194/amt-11-4763-2018, 2018.
- Bianchi, F., Kurten, T., Riva, M., Mohr, C., Rissanen, M. P., Roldin, P., Berndt, T., Crounse, J. D., Wennberg, P. O., Mentel, T. F., Wildt, J., Junninen, H., Jokinen, T., Kulmala, M., Worsnop, D. R., Thornton, J. A., Donahue, N., Kjaergaard, H. G., and Ehn, M.: Highly Oxygenated Organic Molecules (HOM) from Gas-Phase Autoxidation Involving Peroxy Radicals: A Key Contributor to Atmospheric Aerosol, *Chem. Rev.*, 119, 3472-3509, 10.1021/acs.chemrev.8b00395, 2019.
- Boyd, C. M., Sanchez, J., Xu, L., Eugene, A. J., Nah, T., Tuet, W. Y., Guzman, M. I., and Ng, N. L.: Secondary organic aerosol formation from the beta-pinene+ $\text{NO}_3$  system: effect of humidity and peroxy radical fate, *Atmos. Chem. Phys.*, 15, 7497-7522, 10.5194/acp-15-7497-2015, 2015.
- Boyd, C. M., Nah, T., Xu, L., Berkemeier, T., and Ng, N. L.: Secondary Organic Aerosol (SOA) from Nitrate Radical Oxidation of Monoterpenes: Effects of Temperature, Dilution, and Humidity on Aerosol Formation, Mixing, and Evaporation, *Environ. Sci. Technol.*, 51, 7831-7841, 10.1021/acs.est.7b01460, 2017.
- Brown, S. S., deGouw, J. A., Warneke, C., Ryerson, T. B., Dube, W. P., Atlas, E., Weber, R. J., Peltier, R. E., Neuman, J. A., Roberts, J. M., Swanson, A., Flocke, F., McKeen, S. A., Brioude, J., Sommariva, R., Trainer, M., Fehsenfeld, F. C., and Ravishankara, A. R.: Nocturnal isoprene oxidation over the Northeast United States in summer and its impact on reactive nitrogen partitioning and secondary organic aerosol, *Atmos. Chem. Phys.*, 9, 3027-3042, 10.5194/acp-9-3027-2009, 2009.
- Brown, S. S., Dube, W. P., Peischl, J., Ryerson, T. B., Atlas, E., Warneke, C., de Gouw, J. A., Hekkert, S. t. L., Brock, C. A., Flocke, F., Trainer, M., Parrish, D. D., Fehsenfeld, F. C., and Ravishankara, A. R.: Budgets for nocturnal VOC oxidation by nitrate radicals aloft during the 2006 Texas Air Quality Study, *J. Geophys. Res.-Atmos.*, 116, 10.1029/2011jd016544, 2011.
- Brown, S. S., and Stutz, J.: Nighttime radical observations and chemistry, *Chem. Soc. Rev.*, 41, 6405-6447, 10.1039/c2cs35181a, 2012.

Chen, J., Møller, K. H., Wennberg, P. O., and Kjaergaard, H. G.: Unimolecular Reactions Following Indoor and Outdoor Limonene Ozonolysis, *J. Phys. Chem. A* 125, 669-680, 10.1021/acs.jpca.0c09882, 2021.

Chen, Y. L., Takeuchi, M., Nah, T., Xu, L., Canagaratna, M. R., Stark, H., Baumann, K., Canonaco, F., Prevot, A. S. H., Huey, L. G., Weber, R. J., and Ng, N. L.: Chemical characterization of secondary organic aerosol at a rural site in the southeastern US: insights from simultaneous high-resolution time-of-flight aerosol mass spectrometer (HR-ToF-AMS) and FIGAERO chemical ionization mass spectrometer (CIMS) measurements, *Atmos. Chem. Phys.*, 20, 8421-8440, 10.5194/acp-20-8421-2020, 2020.

Claflin, M. S., and Ziemann, P. J.: Identification and Quantitation of Aerosol Products of the Reaction of  $\beta$ -Pinene with  $\text{NO}_3$  Radicals and Implications for Gas- and Particle-Phase Reaction Mechanisms, *The Journal of Physical Chemistry A*, 122, 3640-3652, 10.1021/acs.jpca.8b00692, 2018.

Crounse, J. D., Knap, H. C., Ørnsø, K. B., Jørgensen, S., Paulot, F., Kjaergaard, H. G., and Wennberg, P. O.: Atmospheric Fate of Methacrolein. 1. Peroxy Radical Isomerization Following Addition of OH and  $\text{O}_2$ , *The Journal of Physical Chemistry A*, 116, 5756-5762, 10.1021/jp211560u, 2012.

Crounse, J. D., Nielsen, L. B., Jørgensen, S., Kjaergaard, H. G., and Wennberg, P. O.: Autoxidation of Organic Compounds in the Atmosphere, *J. Phys. Chem. Lett.*, 4, 3513-3520, 10.1021/jz4019207, 2013.

Draper, D. C., Myllys, N., Hyttinen, N., Møller, K. H., Kjaergaard, H. G., Fry, J. L., Smith, J. N., and Kurten, T.: Formation of Highly Oxidized Molecules from  $\text{NO}_3$  Radical Initiated Oxidation of Delta-3-Carene: A Mechanistic Study, *Acs Earth and Space Chemistry*, 3, 1460-1470, 10.1021/acsearthspacechem.9b00143, 2019.

Ehn, M., Thornton, J. A., Kleist, E., Sipila, M., Junninen, H., Pullinen, I., Springer, M., Rubach, F., Tillmann, R., Lee, B., Lopez-Hilfiker, F., Andres, S., Acir, I. H., Rissanen, M., Jokinen, T., Schobesberger, S., Kangasluoma, J., Kontkanen, J., Nieminen, T., Kurten, T., Nielsen, L. B., Jørgensen, S., Kjaergaard, H. G., Canagaratna, M., Dal Maso, M., Berndt, T., Petaja, T., Wahner, A., Kerminen, V. M., Kulmala, M., Worsnop, D. R., Wildt, J., and Mentel, T. F.: A large source of low-volatility secondary organic aerosol, *Nature*, 506, 476-479, 10.1038/nature13032, 2014.

Ehn, M., Berndt, T., Wildt, J., and Mentel, T.: Highly Oxygenated Molecules from Atmospheric Autoxidation of Hydrocarbons: A Prominent Challenge for Chemical Kinetics Studies, *Int. J. Chem. Kinet.*, 49, 821-831, 10.1002/kin.21130, 2017.

Eisele, F. L., and Tanner, D. J.: Measurement of the gas phase concentration of  $\text{H}_2\text{SO}_4$  and methane sulfonic acid and estimates of  $\text{H}_2\text{SO}_4$  production and loss in the atmosphere, 98, 9001-9010, 10.1029/93jd00031, 1993.

Faxon, C., Hammes, J., Le Breton, M., Pathak, R. K., and Hallquist, M.: Characterization of organic nitrate constituents of secondary organic aerosol (SOA) from nitrate-radical-initiated oxidation of limonene using high-resolution chemical ionization mass spectrometry, *Atmos. Chem. Phys.*, 18, 5467-5481, 10.5194/acp-18-5467-2018, 2018.

Finlayson-Pitts, B., and Pitts, J.: Chemistry of the upper and lower atmosphere, Academic Press, San Diego, 2000.

Fry, J. L., Kiendler-Scharr, A., Rollins, A. W., Wooldridge, P. J., Brown, S. S., Fuchs, H., Dube, W., Mensah, A., dal Maso, M., Tillmann, R., Dorn, H. P., Brauers, T., and Cohen, R. C.: Organic nitrate and secondary organic aerosol yield from  $\text{NO}_3$  oxidation of beta-pinene evaluated using a gas-phase kinetics/aerosol partitioning model, *Atmos. Chem. Phys.*, 9, 1431-1449, 2009.

Fry, J. L., Kiendler-Scharr, A., Rollins, A. W., Brauers, T., Brown, S. S., Dorn, H. P., Dube, W. P., Fuchs, H., Mensah, A., Rohrer, F., Tillmann, R., Wahner, A., Wooldridge, P. J., and Cohen, R. C.: SOA from limonene: role of  $\text{NO}_3$  in its generation and degradation, *Atmos. Chem. Phys.*, 11, 3879-3894, 10.5194/acp-11-3879-2011, 2011.

Fry, J. L., Draper, D. C., Barsanti, K. C., Smith, J. N., Ortega, J., Winkle, P. M., Lawler, M. J., Brown, S. S., Edwards, P. M., Cohen, R. C., and Lee, L.: Secondary Organic Aerosol Formation and Organic Nitrate Yield from  $\text{NO}_3$  Oxidation of Biogenic Hydrocarbons, *Environ. Sci. Technol.*, 48, 11944-11953, 10.1021/es502204x, 2014.

Fry, J. L., Brown, S. S., Middlebrook, A. M., Edwards, P. M., Campuzano-Jost, P., Day, D. A., Jimenez, J. L., Allen, H. M., Ryerson, T. B., Pollack, I., Graus, M., Warneke, C., de Gouw, J. A., Brock, C. A., Gilman, J., Lerner, B. M., Dube, W. P., Liao, J., and Welti, A.: Secondary organic aerosol (SOA) yields from  $\text{NO}_3$  radical + isoprene based on nighttime aircraft power plant plume transects, *Atmos. Chem. Phys.*, 18, 11663-11682, 10.5194/acp-18-11663-2018, 2018.

Fuchs, H., Dorn, H. P., Bachner, M., Bohn, B., Brauers, T., Gomm, S., Hofzumahaus, A., Holland, F., Nehr, S., Rohrer, F., Tillmann, R., and Wahner, A.: Comparison of OH concentration measurements by DOAS and LIF during SAPHIR chamber experiments at high OH reactivity and low NO concentration, *Atmos. Meas. Tech.*, 5, 1611-1626, 10.5194/amt-5-1611-2012, 2012.

Garmash, O., Rissanen, M. P., Pullinen, I., Schmitt, S., Kausiala, O., Tillmann, R., Percival, C., Bannan, T. J., Priestley, M., Hallquist, Å. M., Kleist, E., Kiendler-Scharr, A., Hallquist, M., Berndt, T., McFiggans, G., Wildt, J., Mentel, T., and Ehn, M.: Multi-generation OH oxidation as a source for highly oxygenated organic molecules from aromatics, *Atmos. Chem. Phys. Discuss.*, 2019, 1-33, 10.5194/acp-2019-582, 2019.

Geyer, A., Alicke, B., Konrad, S., Schmitz, T., Stutz, J., and Platt, U.: Chemistry and oxidation capacity of the nitrate radical in the continental boundary layer near Berlin, *J. Geophys. Res.-Atmos.*, 106, 8013-8025, 10.1029/2000jd900681, 2001.

Hamilton, J. F., Bryant, D. J., Edwards, P. M., Ouyang, B., Bannan, T. J., Mehra, A., Mayhew, A. W., Hopkins, J. R., Dunmore, R. E., Squires, F. A., Lee, J. D., Newland, M. J., Worrall, S. D., Bacak, A., Coe, H., Percival, C., Whalley, L. K., Heard, D. E., Slater, E. J., Jones, R. L., Cui, T., Surratt, J. D., Reeves, C. E., Mills, G. P., Grimmond, S., Sun, Y., Xu, W., Shi, Z., and Rickard, A. R.: Key Role of  $\text{NO}_3$  Radicals in the Production of Isoprene Nitrates and Nitrooxyorganosulfates in Beijing, *Environ. Sci. Technol.*, 55, 842-853, 10.1021/acs.est.0c05689, 2021.

Huang, W., Saathoff, H., Shen, X. L., Ramisetty, R., Leisner, T., and Mohr, C.: Chemical Characterization of Highly Functionalized Organonitrates Contributing to Night-Time Organic Aerosol Mass Loadings and Particle Growth, *Environ. Sci. Technol.*, 53, 1165-1174, 10.1021/acs.est.8b05826, 2019.

Hyttinen, N., Kupiainen-Määttä, O., Rissanen, M. P., Muuronen, M., Ehn, M., and Kurtén, T.: Modeling the Charging of Highly Oxidized Cyclohexene Ozonolysis Products Using Nitrate-Based Chemical Ionization, *The Journal of Physical Chemistry A*, 119, 6339-6345, 10.1021/acs.jpca.5b01818, 2015.

Japar, S. M., and Niki, H.: Gas-phase reactions of the nitrate radical with olefins, *The Journal of Physical Chemistry*, 79, 1629-1632, 10.1021/j100583a002, 1975.

Jenkin, M. E., Saunders, S. M., and Pilling, M. J.: The tropospheric degradation of volatile organic compounds: A protocol for mechanism development, *Atmos. Environ.*, 31, 81-104, 10.1016/s1352-2310(96)00105-7, 1997.

Jenkin, M. E., Boyd, A. A., and Lesclaux, R.: Peroxy Radical Kinetics Resulting from the OH-Initiated Oxidation of 1,3-Butadiene, 2,3-Dimethyl-1,3-Butadiene and Isoprene, *J. Atmos. Chem.*, 29, 267-298, 10.1023/A:1005940332441, 1998.

Jenkin, M. E., Saunders, S. M., Wagner, V., and Pilling, M. J.: Protocol for the development of the Master Chemical Mechanism, MCM v3 (Part B): tropospheric degradation of aromatic volatile organic compounds, *Atmos. Chem. Phys.*, 3, 181-193, 2003.

Jenkin, M. E., Young, J. C., and Rickard, A. R.: The MCM v3.3.1 degradation scheme for isoprene, *Atmos. Chem. Phys.*, 15, 11433-11459, 10.5194/acp-15-11433-2015, 2015.

Jokinen, T., Sipila, M., Junninen, H., Ehn, M., Lonn, G., Hakala, J., Petaja, T., Mauldin, R. L., III, Kulmala, M., and Worsnop, D. R.: Atmospheric sulphuric acid and neutral cluster measurements using CI-APi-TOF, *Atmos. Chem. Phys.*, 12, 4117-4125, 10.5194/acp-12-4117-2012, 2012.

Jokinen, T., Sipila, M., Richters, S., Kerminen, V. M., Paasonen, P., Stratmann, F., Worsnop, D., Kulmala, M., Ehn, M., Herrmann, H., and Berndt, T.: Rapid Autoxidation Forms Highly Oxidized RO<sub>2</sub> Radicals in the Atmosphere, *Angew. Chem.-Int. Edit.*, 53, 14596-14600, 10.1002/anie.201408566, 2014.

Jokinen, T., Berndt, T., Makkonen, R., Kerminen, V. M., Junninen, H., Paasonen, P., Stratmann, F., Herrmann, H., Guenther, A. B., Worsnop, D. R., Kulmala, M., Ehn, M., and Sipila, M.: Production of extremely low volatile organic compounds from biogenic emissions: Measured yields and atmospheric implications, *Proc. Nat. Acad. Sci. U.S.A.*, 112, 7123-7128, 10.1073/pnas.1423977112, 2015.

Kaminski, M., Fuchs, H., Acir, I.-H., Bohn, B., Brauers, T., Dorn, H.-P., Haeseler, R., Hofzumahaus, A., Li, X., Lutz, A., Nehr, S., Rohrer, F., Tillmann, R., Vereecken, L., Wegener, R., and Wahner, A.: Investigation of the beta-pinene photooxidation by OH in the atmosphere simulation chamber SAPHIR, *Atmos. Chem. Phys.*, 17, 6631-6650, 10.5194/acp-17-6631-2017, 2017.

Kenseth, C. M., Huang, Y. L., Zhao, R., Dalleska, N. F., Hethcox, C., Stoltz, B. M., and Seinfeld, J. H.: Synergistic O<sub>3</sub> + OH oxidation pathway to extremely low-volatility dimers revealed in beta-pinene secondary organic aerosol, *Proc. Nat. Acad. Sci. U.S.A.*, 115, 8301-8306, 10.1073/pnas.1804671115, 2018.

Kirkby, J., Duplissy, J., Sengupta, K., Frege, C., Gordon, H., Williamson, C., Heinritzi, M., Simon, M., Yan, C., Almeida, J., Tröstl, J., Nieminen, T., Ortega, I. K., Wagner, R., Adamov, A., Amorim, A., Bernhammer, A.-K., Bianchi, F., Breitenlechner, M., Brilke, S., Chen, X., Craven, J., Dias, A., Ehrhart, S., Flagan, R. C., Franchin, A., Fuchs, C., Guida, R., Hakala, J., Hoyle, C. R., Jokinen, T., Junninen, H., Kangasluoma, J., Kim, J., Krapf, M., Kürten, A., Laaksonen, A., Lehtipalo, K., Makhmutov, V., Mathot, S., Molteni, U., Onnela, A., Peräkylä, O., Piel, F., Petäjä, T., Praplan, A. P., Pringle, K., Rap, A., Richards, N. A. D., Riipinen, I., Rissanen, M. P., Rondo, L., Sarnela, N., Schobesberger, S., Scott, C. E., Seinfeld, J. H., Sipilä, M., Steiner, G., Stozhkov, Y., Stratmann, F., Tomé, A., Virtanen, A., Vogel, A. L., Wagner, A. C., Wagner, P. E., Weingartner, E., Wimmer, D., Winkler, P. M., Ye, P., Zhang, X., Hansel, A., Dommen, J., Donahue, N. M., Worsnop, D. R., Baltensperger, U., Kulmala, M., Carslaw, K. S., and Curtius, J.: Ion-induced nucleation of pure biogenic particles, *Nature*, 533, 521-526, 10.1038/nature17953, 2016.

Krechmer, J. E., Coggon, M. M., Massoli, P., Nguyen, T. B., Crounse, J. D., Hu, W. W., Day, D. A., Tyndall, G. S., Henze, D. K., Rivera-Rios, J. C., Nowak, J. B., Kimmel, J. R., Mauldin, R. L., Stark, H., Jayne, J. T., Sipila, M., Junninen, H., St Clair, J. M., Zhang, X., Feiner, P. A., Zhang, L., Miller, D. O., Brune, W. H., Keutsch, F. N., Wennberg, P. O., Seinfeld, J. H., Worsnop, D. R., Jimenez, J. L., and Canagaratna, M. R.: Formation of Low Volatility Organic Compounds and Secondary Organic Aerosol from Isoprene Hydroxyhydroperoxide Low-NO Oxidation, *Environ. Sci. Technol.*, 49, 10330-10339, 10.1021/acs.est.5b02031, 2015.

Kwan, A. J., Chan, A. W. H., Ng, N. L., Kjaergaard, H. G., Seinfeld, J. H., and Wennberg, P. O.: Peroxy radical chemistry and OH radical production during the NO<sub>3</sub>-initiated oxidation of isoprene, *Atmos. Chem. Phys.*, 12, 7499-7515, 10.5194/acp-12-7499-2012, 2012.

Lai, C. C., and Finlayson-Pitts, B. J.: Reactions of dinitrogen pentoxide and nitrogen-dioxide with 1-palmitoyl-2-oleoyl-sn-glycero-3-phosphocholine, *Lipids*, 26, 306-314, 10.1007/bf02537142, 1991.

Lee, B. H., Mohr, C., Lopez-Hilfiker, F. D., Lutz, A., Hallquist, M., Lee, L., Romer, P., Cohen, R. C., Iyer, S., Kurten, T., Hu, W., Day, D. A., Campuzano-Jost, P., Jimenez, J. L., Xu, L., Ng, N. L., Guo, H., Weber, R. J., Wild, R. J., Brown, S. S., Koss, A., de Gouw, J., Olson, K., Goldstein, A. H., Seco, R., Kim, S., McAvey, K., Shepson, P. B., Starn, T., Baumann, K., Edgerton, E. S., Liu, J., Shilling, J. E., Miller, D. O., Brune, W., Schobesberger, S., D'Ambro, E. L., and Thornton, J. A.: Highly functionalized organic nitrates in the southeast United States: Contribution to secondary organic aerosol and reactive nitrogen budgets, *Proc. Nat. Acad. Sci. U.S.A.*, 113, 1516-1521, 10.1073/pnas.1508108113, 2016.

Lu, K. D., Rohrer, F., Holland, F., Fuchs, H., Brauers, T., Oebel, A., Dlugi, R., Hu, M., Li, X., Lou, S. R., Shao, M., Zhu, T., Wahner, A., Zhang, Y. H., and Hofzumahaus, A.: Nighttime observation and chemistry of HO<sub>x</sub> in the Pearl River Delta and Beijing in summer 2006, *Atmos. Chem. Phys.*, 14, 4979-4999, 10.5194/acp-14-4979-2014, 2014.

Malkin, T. L., Goddard, A., Heard, D. E., and Seakins, P. W.: Measurements of OH and HO<sub>2</sub> yields from the gas phase ozonolysis of isoprene, *Atmos. Chem. Phys.*, 10, 1441-1459, 10.5194/acp-10-1441-2010, 2010.

Massoli, P., Stark, H., Canagaratna, M. R., Krechmer, J. E., Xu, L., Ng, N. L., Mauldin, R. L., Yan, C., Kimmel, J., Misztal, P. K., Jimenez, J. L., Jayne, J. T., and Worsnop, D. R.: Ambient Measurements of Highly Oxidized Gas-Phase Molecules during the Southern Oxidant and Aerosol Study (SOAS) 2013, *ACS Earth and Space Chemistry*, 2, 653-672, 10.1021/acsearthspacechem.8b00028, 2018.

McFiggans, G., Mentel, T. F., Wildt, J., Pullinen, I., Kang, S., Kleist, E., Schmitt, S., Springer, M., Tillmann, R., Wu, C., Zhao, D., Hallquist, M., Faxon, C., Le Breton, M., Hallquist, Å. M., Simpson, D., Bergström, R., Jenkin, M. E., Ehn, M., Thornton, J. A., Alfarra, M. R., Bannan, T. J., Percival, C. J., Priestley, M., Topping, D., and Kiendler-Scharr, A.: Secondary organic aerosol reduced by mixture of atmospheric vapours, *Nature*, 565, 587-593, 10.1038/s41586-018-0871-y, 2019.

Mentel, T. F., Springer, M., Ehn, M., Kleist, E., Pullinen, I., Kurten, T., Rissanen, M., Wahner, A., and Wildt, J.: Formation of highly oxidized multifunctional compounds: autoxidation of peroxy radicals formed in the ozonolysis of alkenes - deduced from structure-product relationships, *Atmos. Chem. Phys.*, 15, 6745-6765, 10.5194/acp-15-6745-2015, 2015.

Møller, K. H., Bates, K. H., and Kjaergaard, H. G.: The Importance of Peroxy Radical Hydrogen-Shift Reactions in Atmospheric Isoprene Oxidation, *J. Phys. Chem. A* 123, 920-932, 10.1021/acs.jpca.8b10432, 2019.

Molteni, U., Bianchi, F., Klein, F., El Haddad, I., Frege, C., Rossi, M. J., Dommen, J., and Baltensperger, U.: Formation of highly oxygenated organic molecules from aromatic compounds, *Atmos. Chem. Phys.*, 18, 1909-1921, 10.5194/acp-18-1909-2018, 2018.

Molteni, U., Simon, M., Heinritzi, M., Hoyle, C. R., Bernhammer, A. K., Bianchi, F., Breitenlechner, M., Brilke, S., Dias, A., Duplissy, J., Frege, C., Gordon, H., Heyn, C., Jokinen, T., Kurten, A., Lehtipalo, K., Makhmutov, V., Petaja, T., Pieber, S. M., Praplan, A. P., Schobesberger, S., Steiner, G., Stozhkov, Y., Tome, A., Trostl, J., Wagner, A. C., Wagner, R., Williamson, C., Yan, C., Baltensperger, U., Curtius, J., Donahue, N. M., Hansel, A., Kirkby, J., Kulmala, M., Worsnop, D. R., and Dommen, J.: Formation of Highly Oxygenated Organic Molecules from alpha-Pinene Ozonolysis: Chemical Characteristics, Mechanism, and Kinetic Model Development, *Acs Earth and Space Chemistry*, 3, 873-883, 10.1021/acsearthspacechem.9b00035, 2019.

Nah, T., Sanchez, J., Boyd, C. M., and Ng, N. L.: Photochemical Aging of alpha-pinene and beta-pinene Secondary Organic Aerosol formed from Nitrate Radical Oxidation, *Environ. Sci. Technol.*, 50, 222-231, 10.1021/acs.est.5b04594, 2016.

Ng, N. L., Kwan, A. J., Surratt, J. D., Chan, A. W. H., Chhabra, P. S., Sorooshian, A., Pye, H. O. T., Crounse, J. D., Wennberg, P. O., Flagan, R. C., and Seinfeld, J. H.: Secondary organic aerosol (SOA) formation from reaction of isoprene with nitrate radicals (NO<sub>3</sub>), *Atmos. Chem. Phys.*, 8, 4117-4140, 10.5194/acp-8-4117-2008, 2008.

Nguyen, T. B., Tyndall, G. S., Crounse, J. D., Teng, A. P., Bates, K. H., Schwantes, R. H., Coggon, M. M., Zhang, L., Feiner, P., Milller, D. O., Skog, K. M., Rivera-Rios, J. C., Dorris, M., Olson, K. F., Koss, A., Wild, R. J., Brown, S. S., Goldstein, A. H., de Gouw, J. A., Brune, W. H., Keutsch, F. N., Seinfeldcj, J. H., and Wennberg, P. O.: Atmospheric fates of Criegee intermediates in the ozonolysis of isoprene, *Phys. Chem. Chem. Phys.*, 18, 10241-10254, 10.1039/c6cp00053c, 2016.

Novelli, A., Cho, C., Fuchs, H., Hofzumahaus, A., Rohrer, F., Tillmann, R., Kiendler-Scharr, A., Wahner, A., and Vereecken, L.: Experimental and theoretical study on the impact of a nitrate group on the chemistry of alkoxy radicals, *Phys. Chem. Chem. Phys.*, 23, 5474-5495, 10.1039/D0CP05555G, 2021.

Nozière, B., and Vereecken, L.: Direct Observation of Aliphatic Peroxy Radical Autoxidation and Water Effects: An Experimental and Theoretical Study, *Angew. Chem.-Int. Edit.*, 58, 13976-13982, 10.1002/anie.201907981, 2019.

Perring, A. E., Wisthaler, A., Graus, M., Wooldridge, P. J., Lockwood, A. L., Mielke, L. H., Shepson, P. B., Hansel, A., and Cohen, R. C.: A product study of the isoprene+NO<sub>3</sub> reaction, *Atmos. Chem. Phys.*, 9, 4945-4956, 10.5194/acp-9-4945-2009, 2009.

Pfrang, C., Martin, R. S., Canosa-Mas, C. E., and Wayne, R. P.: Gas-phase reactions of NO<sub>3</sub> and N<sub>2</sub>O<sub>5</sub> with (Z)-hex-4-en-1-ol, (Z)-hex-3-en-1-ol ('leaf alcohol'), (E)-hex-3-en-1-ol, (Z)-hex-2-en-1-ol and (E)-hex-2-en-1-ol, *Phys. Chem. Chem. Phys.*, 8, 354-363, 10.1039/b510835g, 2006.

Pullinen, I., Schmitt, S., Kang, S., Sarrafzadeh, M., Schlag, P., Andres, S., Kleist, E., Mentel, T. F., Rohrer, F., Springer, M., Tillmann, R., Wildt, J., Wu, C., Zhao, D., Wahner, A., and Kiendler-Scharr, A.: Impact of NO<sub>x</sub> on secondary organic aerosol (SOA) formation from  $\alpha$ -pinene and  $\beta$ -pinene photooxidation: the role of highly oxygenated organic nitrates, *Atmos. Chem. Phys.*, 20, 10125-10147, 10.5194/acp-20-10125-2020, 2020.

Quelever, L. L. J., Kristensen, K., Jensen, L. N., Rosati, B., Teiwes, R., Daellenbach, K. R., Perakyla, O., Roldin, P., Bossi, R., Pedersen, H. B., Glasius, M., Bilde, M., and Ehn, M.: Effect of temperature on the formation of highly oxygenated organic molecules (HOMs) from alpha-pinene ozonolysis, *Atmos. Chem. Phys.*, 19, 7609-7625, 10.5194/acp-19-7609-2019, 2019.

Richters, S., Pfeifle, M., Olzmann, M., and Berndt, T.: endo-Cyclization of unsaturated RO<sub>2</sub> radicals from the gas-phase ozonolysis of cyclohexadienes, *Chem. Commun.*, 53, 4132-4135, 10.1039/c7cc01350g, 2017.

Rissanen, M. P., Kurten, T., Sipila, M., Thornton, J. A., Kangasluoma, J., Sarnela, N., Junninen, H., Jørgensen, S., Schallhart, S., Kajos, M. K., Taipale, R., Springer, M., Mentel, T. F., Ruuskanen, T., Petaja, T., Worsnop, D. R., Kjaergaard, H. G., and Ehn, M.: The Formation of Highly Oxidized Multifunctional Products in the Ozonolysis of Cyclohexene, *J. Am. Chem. Soc.*, 136, 15596-15606, 10.1021/ja507146s, 2014.

Rissanen, M. P., Kurten, T., Sipila, M., Thornton, J. A., Kausala, O., Garmash, O., Kjaergaard, H. G., Petaja, T., Worsnop, D. R., Ehn, M., and Kulmala, M.: Effects of Chemical Complexity on the Autoxidation Mechanisms of Endocyclic Alkene Ozonolysis Products: From Methylcyclohexenes toward Understanding alpha-Pinene, *J. Phys. Chem. A* 119, 4633-4650, 10.1021/jp510966g, 2015.

Riva, M., Rantala, P., Krechmer, J. E., Perakyla, O., Zhang, Y. J., Heikkinen, L., Garmash, O., Yan, C., Kulmala, M., Worsnop, D., and Ehn, M.: Evaluating the performance of five different chemical ionization techniques for detecting gaseous oxygenated organic species, *Atmos. Meas. Tech.*, 12, 2403-2421, 10.5194/amt-12-2403-2019, 2019.

Rohrer, F., Bohn, B., Brauers, T., Bruning, D., Johnen, F. J., Wahner, A., and Kleffmann, J.: Characterisation of the photolytic HONO-source in the atmosphere simulation chamber SAPHIR, *Atmos. Chem. Phys.*, 5, 2189-2201, 2005.

Rollins, A. W., Kiendler-Scharr, A., Fry, J. L., Brauers, T., Brown, S. S., Dorn, H. P., Dube, W. P., Fuchs, H., Mensah, A., Mentel, T. F., Rohrer, F., Tillmann, R., Wegener, R., Wooldridge, P. J., and Cohen, R. C.: Isoprene oxidation by nitrate radical: alkyl nitrate and secondary organic aerosol yields, *Atmos. Chem. Phys.*, 9, 6685-6703, 2009.

Saunders, S. M., Jenkin, M. E., Derwent, R. G., and Pilling, M. J.: Protocol for the development of the Master Chemical Mechanism, MCM v3 (Part A): tropospheric degradation of non-aromatic volatile organic compounds, *Atmos. Chem. Phys.*, 3, 161-180, 2003.

Schwantes, R. H., Teng, A. P., Nguyen, T. B., Coggon, M. M., Crounse, J. D., St Clair, J. M., Zhang, X., Schilling, K. A., Seinfeld, J. H., and Wennberg, P. O.: Isoprene NO<sub>3</sub> Oxidation Products from the RO<sub>2</sub> + HO<sub>2</sub> Pathway, *J. Phys. Chem. A* 119, 10158-10171, 10.1021/acs.jpca.5b06355, 2015.

Skov, H., Hjorth, J., Lohse, C., Jensen, N. R., and Restelli, G.: Products and mechanisms of the reactions of the nitrate radical (NO<sub>3</sub>) with isoprene, 1,3-butadiene and 2,3-dimethyl-1,3-butadiene in air, *Atmospheric Environment. Part A. General Topics*, 26, 2771-2783, [https://doi.org/10.1016/0960-1686\(92\)90015-D](https://doi.org/10.1016/0960-1686(92)90015-D), 1992.

Stark, M. S.: Epoxidation of Alkenes by Peroxyl Radicals in the Gas Phase: Structure–Activity Relationships, *The Journal of Physical Chemistry A*, 101, 8296-8301, 10.1021/jp972054+, 1997.

Stark, M. S.: Addition of Peroxyl Radicals to Alkenes and the Reaction of Oxygen with Alkyl Radicals, *J. Am. Chem. Soc.* , 122, 4162-4170, 10.1021/ja993760m, 2000.

Starn, T. K., Shepson, P. B., Bertman, S. B., Riemer, D. D., Zika, R. G., and Olszyna, K.: Nighttime isoprene chemistry at an urban-impacted forest site, 103, 22437-22447, <https://doi.org/10.1029/98JD01201>, 1998.

Stroud, C. A., Roberts, J. M., Williams, E. J., Hereid, D., Angevine, W. M., Fehsenfeld, F. C., Wisthaler, A., Hansel, A., Martinez-Harder, M., Harder, H., Brune, W. H., Hoenninger, G., Stutz, J., and White, A. B.: Nighttime isoprene trends at an urban forested site during the 1999 Southern Oxidant Study, 107, ACH 7-1-ACH 7-14, <https://doi.org/10.1029/2001JD000959>, 2002.

Takeuchi, M., and Ng, N. L.: Chemical composition and hydrolysis of organic nitrate aerosol formed from hydroxyl and nitrate radical oxidation of alpha-pinene and beta-pinene, *Atmos. Chem. Phys.*, 19, 12749-12766, 10.5194/acp-19-12749-2019, 2019.

Tan, Z. F., Lu, K. D., Hofzumahaus, A., Fuchs, H., Bohn, B., Holland, F., Liu, Y. H., Rohrer, F., Shao, M., Sun, K., Wu, Y. S., Zeng, L. M., Zhang, Y. S., Zou, Q., Kiendler-Scharr, A., Wahner, A., and Zhang, Y. H.: Experimental budgets of OH, HO<sub>2</sub>, and RO<sub>2</sub> radicals and implications for ozone formation in the Pearl River Delta in China 2014, *Atmos. Chem. Phys.*, 19, 7129-7150, 10.5194/acp-19-7129-2019, 2019.

Tröstl, J., Chuang, W. K., Gordon, H., Heinritzi, M., Yan, C., Molteni, U., Ahlm, L., Frege, C., Bianchi, F., Wagner, R., Simon, M., Lehtipalo, K., Williamson, C., Craven, J. S., Duplissy, J., Adamov, A., Almeida, J., Bernhammer, A.-K., Breitenlechner, M., Brilke, S., Dias, A., Ehrhart, S., Flagan, R. C., Franchin, A., Fuchs, C., Guida, R., Gysel, M., Hansel, A., Hoyle, C. R., Jokinen, T., Junninen, H., Kangasluoma, J., Keskinen, H., Kim, J., Krapf, M., Kürten, A., Laaksonen, A., Lawler, M., Leiminger, M., Mathot, S., Möhler, O., Nieminen, T., Onnela, A., Petäjä, T., Piel, F. M., Miettinen, P., Rissanen, M. P., Rondo, L., Sarnela, N., Schobesberger, S., Sengupta, K., Sipilä, M., Smith, J. N., Steiner, G., Tomè, A., Virtanen, A., Wagner, A. C., Weingartner, E., Wimmer, D., Winkler, P. M., Ye, P., Carslaw, K. S., Curtius, J., Dommen, J., Kirkby, J., Kulmala, M., Riipinen, I., Worsnop, D. R., Donahue, N. M., and Baltensperger, U.: The role of low-volatility organic compounds in initial particle growth in the atmosphere, *Nature*, 533, 527-531, 10.1038/nature18271, 2016.

Valiev, R. R., Hasan, G., Salo, V.-T., Kubecka, J., and Kurten, T.: Intersystem Crossings Drive Atmospheric Gas-Phase Dimer Formation, *The journal of physical chemistry. A*, 123, 6596-6604, 10.1021/acs.jpca.9b02559, 2019.

Vereecken, L., and Peeters, J.: Nontraditional (per)oxy ring-closure paths in the atmospheric oxidation of isoprene and monoterpenes, *J. Phys. Chem. A* 108, 5197-5204, 10.1021/jp049219g, 2004.

Vereecken, L., Mueller, J. F., and Peeters, J.: Low-volatility poly-oxygenates in the OH-initiated atmospheric oxidation of alpha-pinene: impact of non-traditional peroxy radical chemistry, *Phys. Chem. Chem. Phys.*, 9, 5241-5248, 10.1039/b708023a, 2007.

Vereecken, L., and Peeters, J.: A structure-activity relationship for the rate coefficient of H-migration in substituted alkoxy radicals, *Phys. Chem. Chem. Phys.*, 12, 12608-12620, 10.1039/c0cp00387e, 2010.

Vereecken, L., and Francisco, J. S.: Theoretical studies of atmospheric reaction mechanisms in the troposphere, *Chem. Soc. Rev.*, 41, 6259-6293, 10.1039/c2cs35070j, 2012.

Vereecken, L., and Peeters, J.: A theoretical study of the OH-initiated gas-phase oxidation mechanism of beta-pinene (C<sub>10</sub>H<sub>16</sub>): first generation products, *Phys. Chem. Chem. Phys.*, 14, 3802-3815, 10.1039/c2cp23711c, 2012.

Vereecken, L., and Nozière, B.: H migration in peroxy radicals under atmospheric conditions, *Atmos. Chem. Phys.*, 20, 7429-7458, 10.5194/acp-20-7429-2020, 2020.

Vereecken, L., Carlsson, P. T. M., Novelli, A., Bernard, F., Brown, S. S., Cho, C., Crowley, J. N., Fuchs, H., Mellouki, W., Reimer, D., Shenolikar, J., Tillmann, R., Zhou, L., Kiendler-Scharr, A., and Wahner, A.: Theoretical and experimental study of peroxy and alkoxy radicals in the NO<sub>3</sub>-initiated oxidation of isoprene, *Phys. Chem. Chem. Phys.*, 23, 5496-5515, 10.1039/d0cp06267g, 2021.

Viggiano, A. A., Seeley, J. V., Mundis, P. L., Williamson, J. S., and Morris, R. A.: Rate Constants for the Reactions of  $\text{XO}_3\text{-}(\text{H}_2\text{O})_n$  (X = C, HC, and N) and  $\text{NO}_3\text{-}(\text{HNO}_3)_n$  with  $\text{H}_2\text{SO}_4$ : Implications for Atmospheric Detection of  $\text{H}_2\text{SO}_4$ , *The Journal of Physical Chemistry A*, 101, 8275-8278, 10.1021/jp971768h, 1997.

Wagner, N. L., Dubé, W. P., Washenfelder, R. A., Young, C. J., Pollack, I. B., Ryerson, T. B., and Brown, S. S.: Diode laser-based cavity ring-down instrument for  $\text{NO}_3$ ,  $\text{N}_2\text{O}_5$ ,  $\text{NO}$ ,  $\text{NO}_2$  and  $\text{O}_3$  from aircraft, *Atmos. Meas. Tech.*, 4, 1227-1240, 10.5194/amt-4-1227-2011, 2011.

Wang, Y., Mehra, A., Krechmer, J. E., Yang, G., Hu, X., Lu, Y., Lambe, A., Canagaratna, M., Chen, J., Worsnop, D., Coe, H., and Wang, L.: Oxygenated products formed from OH-initiated reactions of trimethylbenzene: autoxidation and accretion, *Atmos. Chem. Phys.*, 20, 9563-9579, 10.5194/acp-20-9563-2020, 2020.

Wennberg, P. O., Bates, K. H., Crounse, J. D., Dodson, L. G., McVay, R. C., Mertens, L. A., Nguyen, T. B., Praske, E., Schwantes, R. H., Smarte, M. D., St Clair, J. M., Teng, A. P., Zhang, X., and Seinfeld, J. H.: Gas-Phase Reactions of Isoprene and Its Major Oxidation Products, *Chem. Rev.*, 118, 3337-3390, 10.1021/acs.chemrev.7b00439, 2018.

Wu, R., Vereecken, L., Tsiligiannis, E., Kang, S., Albrecht, S. R., Hantschke, L., Zhao, D., Novelli, A., Fuchs, H., Tillmann, R., Hohaus, T., Carlsson, P. T. M., Shenolikar, J., Bernard, F., Crowley, J. N., Fry, J. L., Brownwood, B., Thornton, J. A., Brown, S. S., Kiendler-Scharr, A., Wahner, A., Hallquist, M., and Mentel, T. F.: Molecular composition and volatility of multi-generation products formed from isoprene oxidation by nitrate radical, *Atmos. Chem. Phys. Discuss.*, 2020, 1-37, 10.5194/acp-2020-1180, 2020.

Xu, L., Guo, H. Y., Boyd, C. M., Klein, M., Bougiatioti, A., Cerully, K. M., Hite, J. R., Isaacman-VanWertz, G., Kreisberg, N. M., Knote, C., Olson, K., Koss, A., Goldstein, A. H., Hering, S. V., de Gouw, J., Baumann, K., Lee, S. H., Nenes, A., Weber, R. J., and Ng, N. L.: Effects of anthropogenic emissions on aerosol formation from isoprene and monoterpenes in the southeastern United States, *Proc. Nat. Acad. Sci. U.S.A.*, 112, 37-42, 10.1073/pnas.1417609112, 2015.

Xu, Z. N., Nie, W., Liu, Y. L., Sun, P., Huang, D. D., Yan, C., Krechmer, J., Ye, P. L., Xu, Z., Qi, X. M., Zhu, C. J., Li, Y. Y., Wang, T. Y., Wang, L., Huang, X., Tang, R. Z., Guo, S., Xiu, G. L., Fu, Q. Y., Worsnop, D., Chi, X. G., and Ding, A. J.: Multifunctional Products of Isoprene Oxidation in Polluted Atmosphere and Their Contribution to SOA, 48, e2020GL089276, <https://doi.org/10.1029/2020GL089276>, 2021.

Yan, C., Nie, W., Aijala, M., Rissanen, M. P., Canagaratna, M. R., Massoli, P., Junninen, H., Jokinen, T., Sarnela, N., Hame, S. A. K., Schobesberger, S., Canonaco, F., Yao, L., Prevot, A. S. H., Petaja, T., Kulmala, M., Sipila, M., Worsnop, D. R., and Ehn, M.: Source characterization of highly oxidized multifunctional compounds in a boreal forest environment using positive matrix factorization, *Atmos. Chem. Phys.*, 16, 12715-12731, 10.5194/acp-16-12715-2016, 2016.

Yan, C., Nie, W., Vogel, A. L., Dada, L., Lehtipalo, K., Stolzenburg, D., Wagner, R., Rissanen, M. P., Xiao, M., Ahonen, L., Fischer, L., Rose, C., Bianchi, F., Gordon, H., Simon, M., Heinritzi, M., Garmash, O., Roldin, P., Dias, A., Ye, P., Hofbauer, V., Amorim, A., Bauer, P. S., Bergen, A., Bernhammer, A. K., Breitenlechner, M., Brilke, S., Buchholz, A., Mazon, S. B., Canagaratna, M. R., Chen, X., Ding, A., Dommen, J., Draper, D. C., Duplissy, J., Frege, C., Heyn, C., Guida, R., Hakala, J., Heikkinen, L., Hoyle, C. R., Jokinen, T., Kangasluoma, J., Kirkby, J., Kontkanen, J., Kurten, A., Lawler, M. J., Mai, H., Mathot, S., Mauldin, R. L., Molteni, U., Nichman, L., Nieminen, T., Nowak, J., Ojdanic, A., Onnela, A., Pajunoja, A., Petaja, T., Piel, F., Quelever, L. L. J., Sarnela, N., Schallhart, S., Sengupta, K., Sipila, M., Tome, A., Trostl, J., Vaisanen, O., Wagner, A. C., Yliisirnio, A., Zha, Q., Baltensperger, U., Carslaw, K. S., Curtius, J., Flagan, R. C., Hansel, A., Riipinen, I., Smith, J. N., Virtanen, A., Winkler, P. M., Donahue, N. M., Kerminen, V. M., Kulmala, M., Ehn, M., and Worsnop, D. R.: Size-dependent influence of  $\text{NO}_x$  on the growth rates of organic aerosol particles, *Science Advances*, 6, 9, 10.1126/sciadv.aay4945, 2020.

Zhao, D. F., Buchholz, A., Kortner, B., Schlag, P., Rubach, F., Kiendler-Scharr, A., Tillmann, R., Wahner, A., Flores, J. M., Rudich, Y., Watne, Å. K., Hallquist, M., Wildt, J., and Mentel, T. F.: Size-dependent hygroscopicity parameter ( $\kappa$ ) and chemical composition of secondary organic cloud condensation nuclei, *Geophys. Res. Lett.*, 42, 10920-10928, 10.1002/2015gl066497, 2015a.

Zhao, D. F., Kaminski, M., Schlag, P., Fuchs, H., Acir, I. H., Bohn, B., Häseler, R., Kiendler-Scharr, A., Rohrer, F., Tillmann, R., Wang, M. J., Wegener, R., Wildt, J., Wahner, A., and Mentel, T. F.: Secondary organic aerosol formation from hydroxyl radical oxidation and ozonolysis of monoterpenes, *Atmos. Chem. Phys.*, 15, 991-1012, 10.5194/acp-15-991-2015, 2015b.

Zhao, D. F., Schmitt, S. H., Wang, M. J., Acir, I. H., Tillmann, R., Tan, Z. F., Novelli, A., Fuchs, H., Pullinen, I., Wegener, R., Rohrer, F., Wildt, J., Kiendler-Scharr, A., Wahner, A., and Mentel, T. F.: Effects of NO<sub>x</sub> and SO<sub>2</sub> on the secondary organic aerosol formation from photooxidation of alpha-pinene and limonene, *Atmos. Chem. Phys.*, 18, 1611-1628, 10.5194/acp-18-1611-2018, 2018.

Ziemann, P. J., and Atkinson, R.: Kinetics, products, and mechanisms of secondary organic aerosol formation, *Chem. Soc. Rev.*, 41, 6582-6605, 10.1039/c2cs35122f, 2012.